Mixing and Segregation of Granular Materials

J. M. Ottino[1] and D. V. Khakhar[2]

[1]Department of Chemical Engineering, Northwestern University, Evanston, Illinois 60203; e-mail: ottino@chem-eng.nwu.edu

[2]Department of Chemical Engineering, Indian Institute of Technology—Bombay Powai, Bombay, 400076; India; e-mail: khakhar@che.iitb.ernet.in

■ **Abstract**   Granular materials segregate. Small differences in either size or density lead to flow-induced segregation, a complex phenomenon without parallel in fluids. Modeling of mixing and segregation processes requires the confluence of several tools, including continuum and discrete descriptions (particle dynamics, Monte Carlo simulations, cellular automata computations) and, often, considerable geometrical insight. None of these viewpoints, however, is wholly satisfactory by itself. Moreover, continuum and discrete descriptions of granular flows are regime dependent, and this fact may require adopting different subviewpoints. This review organizes a body of knowledge that forms—albeit imperfectly—the beginnings of an expandable continuum framework for the description of mixing and segregation of granular materials. We focus primarily on noncohesive particles, possibly differing in size, density, shape, etc. We present segregation mechanisms and models for size and density segregation and introduce chaotic advection, which appears in noncircular tumblers. Chaotic advection interacts in nontrivial ways with segregation in granular materials and leads to unique equilibrium structures that serve as a prototype for systems displaying organization in the midst of disorder.

1. INTRODUCTION

Mixing of granular materials is unquestionably important. The knowledge base, however, is less developed than for fluids (e.g. Ottino 1990) and certainly is not yet at a point where a first-principles modeling attack is either realistic or possible. The picture is far from bleak though, and granular-flow studies have received, over the past few years, substantial and renewed attention within the physics and engineering communities (Jaeger et al 1996a, b, Jaeger & Nagel 1992, Bridgwater 1995). It is true, however, that current engineering approaches attack mixing problems on an ad hoc basis and that extrapolation from existing empirical knowledge is hard. The sources of complications are many.

Granular materials segregate. Small differences in either size or density lead to flow-induced segregation, a phenomenon without parallel in fluids. Segregation of granular materials is a complex and imperfectly understood phenomenon. Segregation issues are, however, unavoidable in practice; industrial formulations are typically multicomponent often requiring multiple mixing steps and which invariably require solving serious segregation-related problems. Design decisions are routinely made without a fundamental understanding of this phenomenon.

The first attempts to describe solid mixing—by developing physical concepts and vocabulary—were based on analogies with fluid mixing. Thus, for example, Lacey (1954) speaks of ''convective mixing,'' ''dispersive mixing,'' and ''shear mixing,'' all in the context of granular flows. Useful analogies are possible (Ottino & Shinbrot 1999). It is apparent, however, that the understanding of mixing of granular matter is more complex than that of regular fluids and that modeling of the mixing of granular materials requires a confluence of several tools, including continuum and discrete descriptions [particle dynamics, Monte Carlo (MC) simulations, and cellular automata calculations] and, often, considerable geometrical insight. None of these viewpoints is wholly satisfactory by itself. Moreover, continuum and discrete descriptions of granular flows are regime dependent, which may require adopting different subviewpoints. The grain inertia regime is dominated by binary collisions. The quasi static regime is characterized by lasting particle contacts (Jackson 1986). MC simulations and cellular automata algorithms are often too idealized to mimic realistic situations. Shortcomings of continuum descriptions manifest on macroscopic scales; particle segregation is an instance in which physical mesoscale processes are imperfectly understood. Although particle dynamics simulations, akin to molecular dynamics (Cundall & Strack 1979), are exact in principle, they require precise physical properties and interaction models, and the results may provide little insight since they are as specific as those originated by a single well-controlled experiment (Cleary et al 1998).

1.1 Coverage

Is there a body of knowledge, however, that can be organized such that it forms—albeit imperfectly—the beginnings of an expandable and coherent framework to describe mixing and segregation of granular materials? We believe that there is, and we try to assemble these viewpoints. We focus primarily on noncohesive particles—possibly differing in size, density, shape, etc—and just one mode of mixing. An examination of current mixing methodologies reveals three main avenues for stirring: shaking, tumbling, and driving impellers or paddles through the granular media. The decision we made here is to focus solely on tumbling. Moreover, within this restricted context, the point of view evolves from simple to complex and adds complications one at a time within a central continuum viewpoint; ad hoc models are not considered. The initial sections examine quasi–two-dimensional flows. Two subcases are considered: slow flow, in which distinct

avalanches occur, and continuous flow, where flow is restricted to a thin, continuously flowing layer, with the rest of the material moving as a solid. Containers are first restricted to circles—which form the base case—and then to ellipses and squares. Continuum and discrete descriptions are interwoven. Segregation is an important element, and this is illustrated by studies in chute flows with MC and particle dynamics (PD) simulations. These studies lead to constitutive equations that can be incorporated into continuum descriptions involving advection, collisional diffusion, and density-/size-driven segregation.

A clarification and caveat are necessary here: the word "particle" is used in two ways—first, as a constituent of granular material, a grain, and, second, in the usual treatment of continuum advection descriptions, for example, following a (primitive) Lagrangian particle $\mathbf{X}$ in a motion $\mathbf{x} = \phi(\mathbf{X},t)$. Now the caveat: unless explicitly stated otherwise, a fluid, typically air, is present. In the cases considered here, lubrication forces become important at length scales below the typical roughness of the particles; thus, the fluid may be safely ignored.

A new element—chaotic advection—which appears in noncircular tumblers, is introduced and developed. The role of collisional diffusion is addressed, and its role in small-scale mixers is highlighted, as well as some of the complex interplays between chaotic advection, which tends to mix, and segregation, which tends to unmix. In the last section we address the role of cohesion, primarily through the role of liquid bridges. A summary of industrial applications concludes the presentation.

Thus, even with a caveat of two-dimensionality, the scenarios are many: (*a*) the container can be circular or noncircular, the second choice giving rise to chaotic advection for continuous flow but not for avalanching flow (see Section 5); (*b*) the container may be filled exactly half way, more than half way, or less than half way [as we shall see, the degree of filling has a pronounced effect on mixing (see Section 5)]; (*c*) the granular matter can consist of identical particles and be nonsegregating, or particles may differ in either density or size, either of which gives rise to segregation; and finally (*d*) the material may be noncohesive (free flowing) or not, and there may be some kind of attractive interaction between grains. Noncohesive particles mix differently than small particles, for which cohesive forces are important (Shinbrot et al 1999, McCarthy & Ottino 1998). Even counting scenario *a* as two choices, *b* as just three, and, in an overly simplistic manner, *d* as just two limiting cases, density and size ratios, there are 72 possibilities for just two flow regimes. It is apparent that this is a remarkably rich subject and that only the outline of possibilities can be sketched here (Figure 1).

2. MIXING FLOWS—STIRRING GRANULAR MATERIALS

The prototypical mixing system is a rotating cylinder. The flow is well defined and can be classified into different regimes (Henein et al 1983, Rajchenbach 1990): at low rotational speeds (quantified in terms of the Froude number, *Fr* =

Container
| CIRCULAR | NON-CIRCULAR |

Degree of Filling
| LESS THAN HALF | EXACTLY HALF | MORE THAN HALF |

Regime
| AVALANCHING | CONTINUOUS |

Granular material
| IDENTICAL POWDERS | DENSITY DIFFERENCES | SIZE DIFFERENCES |

Particle Interactions
| NON-SEGREGATING | SEGREGATING |

Figure 1   Catalog of possible variations in systems in the mixing of granular materials in quasi–two-dimensional mixers.

$\omega L^2/g$, where g is the acceleration due to gravity, L is the length scale of the system, and ω is the rotational speed), the flow comprises discrete avalanches; one stops before the next one begins (the avalanching or slumping regime). At higher speeds a steady flow is obtained with a thin cascading layer at the free surface of the rotating bed (continuous flow, rolling, or cascading regime); if inertial effects are small, the free surface is nearly flat. At still higher speeds, particle inertia effects become important, and particles may become airborne (cataracting regime). $Fr = 1$ corresponds to the critical speed for centrifuging (Figure 2).

In the cases considered here, the flowing material is confined to the avalanching region or the flowing layer, and the rest moves in a solid-body rotation. A simple geometrical model describes the overall flow in the avalanching regime; each avalanche is discrete and comprises a wedge of particles of a specified geometry (Figure 2), which falls to form a geometrically similar wedge at a lower position on the free surface (Metcalfe et al 1995). The details of flow during an avalanche are complex and determine the extent of mixing, which is discussed in more detail in Section 5.1.

Some of the important features of flow in the rolling regime are revealed by Nakagawa et al (1993). They carried out a magnetic resonance imaging study of the flow of mustard seeds, which are nearly spherical. The cascading layer is fluidlike, the velocity profile across the layer is nearly linear (excluding a narrow region of slow deformation near the bed-layer interface), and the average velocity is maximum near the halfway point along the flowing layer. The image analyses studies of Rajchenbach et al (1995) for a two-dimensional system in the region near the midpoint of the layer show similar results.

Analysis of the flow in the layer requires constitutive equations for the transport processes. Kinetic-theory–based continuum models provide such equations
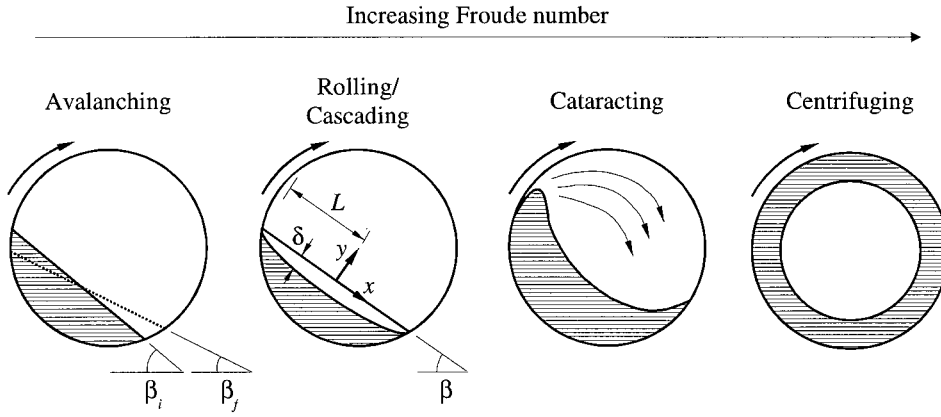
Increasing Froude number

Avalanching   Rolling/Cascading   Cataracting   Centrifuging

Figure 2 Schematic view of flow regimes in a rotating cylinder with increasing rotational speed (ω). In the avalanching regime, the *dashed line* shows the position of the interface after an avalanche, and β_i and β_f are the free surface angles just before and after an avalanche. The angle β in the rolling/cascading or continuous-flow regime is the dynamic or equilibrium angle of repose. The coordinate system is used in the theoretical analysis of Section 2.

for rapid flows of nearly elastic particles and include corrections due to interparticle friction (Lun et al 1984, Johnson & Jackson 1987). The constitutive equations include the granular temperature, which is proportional to the kinetic energy of the velocity fluctuations of the particles. Thus, in addition to continuity and momentum balance equations, a granular thermal-energy equation is required. The results from these models are in good agreement with experimental results for shear flows; however, application of these models to more complex flows, such as the flow in a flowing layer, is not straightforward. Below, we describe a simple approach based on macroscopic balances (transport equations averaged across the layer) that gives reasonable predictions of the flow in the layer.

The simplest tumbling scenario is that of a half-full cylinder. The free surface of the granular material coincides with the diameter of the cylinder and has an exposed surface $-L < x < L$. We assume that the density in the flowing layer is the same as in fixed bed and that the rotational speed is ω. Because in half of a revolution, of duration π/ω, all the material in the cylinder passes through the layer, the volumetric flow rate per unit of cylinder length calculated at the midpoint of the layer ($x = 0$) is

$$Q_0 = \frac{\pi L^2}{2} \frac{1}{(\pi/\omega)} = \frac{\omega L^2}{2}. \tag{1}$$

The average velocity at the midpoint is thus $u(0) = \omega L^2/(2\delta_0)$, where δ_0 is $\delta(0)$.

A more detailed analysis of the velocity field is carried out by Khakhar et al (1997a). Their analysis rests on the kinematical structure of the flow, such that

the inflow and outflow into the flowing layer are determined by the solid-body rotation, and the analysis is most precise when the cylinder is nearly half full. A differential macroscopic-material balance yields that the volume flux Q at point x in the layer is given by (Khakhar et al 1997a)

$$Q_0 = \langle v_x \rangle \delta = \frac{\omega L^2}{2} \left(1 - \frac{x^2}{L^2} \right), \tag{2}$$

where v_x is the velocity along the layer and the pointed brackets denote an average across the layer. The density of the bed and layer are taken to be equal, as above. The analysis to find the average velocity is similar to that of the original analysis by boundary layer theory by Polhausen (1921) and is based on a differential macroscopic momentum balance, in which the velocity field is fed into the equations to determine variation of the average velocity with distance along the layer $[u(x) = \langle v_x \rangle]$. The shear stress at the bed-layer interface is taken to be a sum of the stress from Coulombic friction and the Bagnold (1954) stress $[\sim (dv_x/dy)^2]$ due to collisions. The model has one fitting parameter, the prefactor in Bagnold's stress equation, and it gives good predictions of the layer thickness profiles measured experimentally by flow visualization. The results are nearly independent of the assumed form of the velocity profiles.

A velocity field consistent with the experiments of Nakagawa et al (1993) and Rajchenbach et al (1995) is

$$v_x = 2u \left(1 + \frac{y}{\delta} \right) \tag{3}$$

and

$$v_y = -\omega x \left(\frac{y}{\delta} \right)^2, \tag{4}$$

with Equation 4 obtained by continuity.

Experiments and computational results indicate that the approximation $u \approx u(0)$ is reasonable over most of the layer. With this assumption, Equation 2 yields

$$\delta = \delta_0 \left(1 - \frac{x^2}{L^2} \right), \tag{5}$$

with $u = \omega L^2/(2\delta_0)$ as above.

Elperin & Vikhansky (1998a) developed a similarity solution for the velocity in the layer. They assumed that the stress at the interface is entirely caused by collisions (of Bagnold form) and is equal to a critical value determined by Coulombic friction. Hence the theory also gives the shape of the interface. Predictions of the layer thickness profile are similar to those of Khakhar et al (1997a). A small difference between the two models is that the layer profile of Elperin & Vikhansky (1998a) is symmetric about the midpoint for all parameter values,

whereas that of Khakhar et al (1997a), without the approximation $u \approx u(0)$, is not symmetric.

An experimental result should be mentioned here, because it is important in the modeling of noncircular containers. The ratio δ_0/L remains constant for a constant Froude number. Thus $u \sim L$; the longer the flowing layer, the deeper and faster the flow.

In contrast to fluid flows, granular flows are kinematically defined over most of the flow domain. Shearing of particles is confined to thin layers, while the rest of the particles move as a fixed bed with no relative motion between them. This significantly constrains the variations in flow that can be used to improve mixing; as we see below, however, a byproduct of these kinematical restrictions is that theoretical analyses become simplified. It is also somewhat expected that most of the existing theoretical and experimental attention has been placed on examining surface flows. This is particularly the case for systems with dissimilar particles when segregation accompanies mixing.

3. SURFACE FLOWS—SEGREGATION

Granular mixtures of dissimilar (and not too dissimilar) materials often segregate when they flow or are shaken or vibrated. The most celebrated example of this behavior is the so-called ''Brazil nut'' effect (Williams 1963, Rosato et al 1987), whereby large particles rise to the top of a shaken container of mixed nuts. Other examples are radial segregation (Section 3.2) and axial banding (Section 3.3) in rotating cylinders. Multiple mechanisms have been proposed for these effects. For example, in the Brazil nut effect, the percolation mechanism suggests that small particles can squeeze into small voids below a large particle, but the reverse cannot occur—and, as a result, large particles tend to rise (Rosato et al 1987). Another view—a convection argument—suggests that large particles can rise with the mean flow, but are too large to fit into a narrow down-welling region near the boundary (Knight et al 1993). The percolation argument also applies to flowing layers and may be central in size-driven radial segregation. Particle segregation has attracted substantial interest within the physics community, and there is a considerable body of work in this area, including analysis of segregation during pouring (e.g. Julien & Meakin 1990; Rosato 1999 gives an overview of all aspects of segregation). The discussion below is restricted primarily to shear layers, cylinders, and tumbling and, in particular, to constitutive models that can be incorporated in continuum flow descriptions of mixing and segregation.

3.1 Shear Layer

Consider first a mixture of particles of different sizes flowing in a steady chute flow. For high-solid-volume fractions, the probability of forming a void decreases with increasing void size; large voids are less likely than small voids (Savage &

Lun 1988). Consequently smaller particles are more likely to percolate through such voids to layers below, resulting in a net segregating flux of the smaller particles in the downward direction. Savage & Lun (1988) presented experimental data for polystyrene beads of different sizes in chute flow, in which all the smaller particles collect at the lower levels in the layer, confirming the percolation mechanism described above. The computational results of Hirschfield & Rapaport (1997) for a binary mixture of Lennard-Jones particles with different sizes in a two-dimensional chute flow under gravity showed that large particles rise to the top of the layer. This is in agreement with the results of Savage & Lun (1988). More recent data from Dolgunin & coworkers (1995, 1998) for mixtures with density differences and mixtures with size differences, however, show more complex behavior in which nonmonotonic concentration profiles for the different components are obtained. Theory, discussed below, indicates that a combination of gradients in granular temperature and pressure can produce such concentration profiles.

Drahun & Bridgwater (1983) have carried out an experimental study of a related problem—particle segregation in the formation of a two-dimensional heap. In this case, alternating striations of the different particles are obtained. Quantitative experimental results for the phenomenon are given by Koeppe et al (1998), and an explanation is proposed by Makse et al (1997). Boutreux & de Gennes (1996) have proposed a simple model to describe segregation in surface flows during heap formation.

The specific issue of percolation velocities of small particles in sheared packed beds is addressed by Bridgewater & coworkers (Bridgwater et al 1978, Cooke & Bridgwater 1979, Bridgwater et al 1985). The system comprises a rectangular box with two vertical sides and two sidewalls that can be rotated about hinges at the base. The hinged walls are periodically moved so as to cyclically deform the vertical cross-section from a rectangle to a parallelogram and back to a rectangle. The percolation velocities are found to increase with increasing shear rate and decreasing size of the smaller particles. In contrast to the flowing layer, the particles are in a close-packed configuration in this case, and motion occurs essentially in the failure zones (Bridgwater et al 1985).

3.2 Radial Segregation

A consequence of shear layer segregation in a rotating cylinder is radial segregation, in which denser particles or smaller particles migrate towards the core of the cylinders. The experimental work of Nityanand et al (1986) illustrates the typical behavior of systems with size segregation. At low rotational speeds of the cylinder, percolation dominates, and the smaller particles sink to lower levels in the flowing layer and thus to the inner streamlines of the flow which results in the formation of a core of the smaller particles. However, at higher rotational speeds, the segregation pattern reverses, with the smaller particles at the periphery

instead of the core. These results reflect the complexity of the segregation processes in the layer.

Recent studies of radial segregation have focussed primarily on the dynamics and extent of segregation in the low-rotational-speed regime. Particle dynamics simulations for a two-dimensional system in the rolling regime were used to study the dynamics of segregation due to density differences (Ristow 1994) and size differences (Dury & Ristow 1997). Experimental studies of size segregation in two dimensions have been reported by Clément et al (1995) in the avalanching regime and by Cantelaube & Bideau (1995) in the rolling regime. In both cases the smaller particles formed the central core. Statistics of trapping of the small particles at different points in the layer are reported by Cantelaube & Bideau (1995). Baumann et al (1995) suggested a similar trapping mechanism for size segregation based on computations using a two-dimensional piling algorithm, and Prigozhin & Kalman (1998) have proposed a method for estimating radial segregation based on measurements taken in heap formation. Khakhar et al (1997b) have presented experiments and analysis of simultaneous mixing and segregation for mixtures of equal-sized particles of different density. Alonzos et al (1991) show how a combination of size and density differences can be used to minimize segregation.

3.3 Axial Segregation

Experiments in horizontally placed rotating cylinders containing dissimilar solids, differing either in density or size, reveal alternating axial bands (Donald & Roseman 1962). Here the mechanism, for different-sized particles, is believed to arise from differences in angles of repose of the two materials, which produce small differential axial flows for the two materials (Das Gupta et al 1991, Hill & Kakalios 1995). Experiments show that, if the speed of rotation of the cylinder is large (such that the difference in angles of repose is large), the granular materials segregate into axial bands, whereas at a lower speed (for which the difference is small), the same two materials may mix (Hill & Kakalios 1995). Further, at high rotational speeds, axial segregation may not occur even if there is a difference in the angles of repose because of rapid axial dispersion (Das Gupta et al 1991). The initial growth of the bands is thus a result of the difference between the segregation flux and the axial dispersion (Savage 1993, Zik et al 1994), and an estimate of the former is given by Das Gupta et al (1991). Once the bands are formed, they may grow by fusing with others (Nakagawa 1994). Magnetic resonance imaging of an axially segregated system shows that the initially uniform radial core of the smaller particles becomes varicose, and the bands are the regions where the cross section of the core is the same as that of the bed (Metcalfe & Shattuck 1996, Hill et al 1997). Radial segregation appears to be an important prerequisite of axial segregation. On a long timescale, in long cylinders, traveling wave patterns are obtained (Choo et al 1997). Levitan (1998) developed a model of the long-time behavior of the system that reproduce some of the observations

presented above. The phenomena are, however, complex, and many issues remain imperfectly understood. In fact, the cross-sectional shape of the container has a strong influence on the results (Hill et al 1999a).

4. MODELS FOR DIFFUSIONAL MIXING AND SEGREGATION

As we have seen, the key to segregation lies in large part in the character of the surface flow. Two questions suggest themselves: (*a*) What are the fundamental segregation mechanisms? (*b*) How can these mechanisms be distilled and incorporated into continuum models of mixing of granular flow?

Knowledge about segregation mechanisms can be gained by experiments as well as computations. Computations are of two kinds: PD simulations and MC methods. Before going into a review and analysis of segregation mechanisms, it is convenient to sketch the essential aspects of both methods.

4.1 Monte Carlo Simulations

Monte Carlo simulations may be used to obtain the equilibrium number fraction profiles for a mixture of elastic, hard spheres in a gravitational field. The system is isothermal; that is, the granular temperature of the system is uniform. The system as defined mimics the rapid flow of nearly elastic particles in a chute. Starting from an initially random configuration, the system is driven to equilibrium by means of perturbations which, on the average, either reduce or maintain (at equilibrium) the potential energy of the system. The computational procedure is briefly described below.

Particles, uniformly distributed in the domain initially, are sequentially given random displacements. A displacement is accepted with the probability min $(1, P_{ran})$, if it does not result in overlap with other particles, where

$$P_{\text{ran}} = \exp\left(-\frac{m_t g \Delta z}{T}\right) \quad i = 1 \text{ or } 2, \tag{6}$$

and Δz is the upward vertical component of the displacement, m_i, $i = 1,2$ are the masses of the two types of particles, and g is the acceleration caused by gravity. The number of particles and the volume of the domain are kept constant.

In MC studies of particle segregation by shaking (Rosato et al 1987), the granular temperature is assumed to be vanishingly small ($T \approx 0$), so that initially dispersed particles relax to a quenched (nonequilibrium) state. In contrast, for a flowing layer, a sufficiently high temperature is used so that the particles are in a liquidlike state and can achieve an equilibrium concentration distribution across the layer.

4.2 Particle Dynamics Simulations

Particle dynamics or the discrete element method (Cundall & Strack 1979) is based on the methodology of molecular dynamics for the study of liquids and gases (Allen & Tildesley 1987). This approach is undoubtedly more realistic than the MC method; it is, however, more computationally intensive, and parameter values for interparticle interactions are needed. Geometrical insight into the flow could permit considerable reduction in computational times (McCarthy & Ottino 1997). The bulk flow of the granular material is determined through explicit calculation of the trajectories of each particle (usually spheres) at every time step. Depending on the density and character of the flow to be modeled, different methods of calculating the trajectories are used: a rigid-particle model for low-density, rapid flow—the grain-inertial regime; or a soft-particle model for high-density, slow flow—the quasistatic regime.

In the grain-inertial regime, particle trajectories are found by decomposing the flow into instantaneous binary collisions and applying conservation of linear and angular momentum along with some collision rules. The collision rules generally incorporate inelasticity, through a coefficient of friction, for tangential impact and restitution for normal impact. On the other hand, the quasistatic regime is characterized by lasting particle contacts. For this type of flow, the particle trajectories are obtained via explicit solution of Newton's equations of motion (both for linear and angular momentum) for every particle. Rather than stepping through collisions—as for a rigid particle simulation—in this type of simulation, the particle trajectories are updated at discrete time intervals.

The total force on each particle consists of the gravitational force as well as collision-interparticle forces, which may act either normal or tangent to the line of contact. A description of various force models and their merits can be found in Schafer et al (1996) and McCarthy (1998). The accuracy of a soft-particle simulation is almost wholly dependent on the choice of contact forces—which may act either in the direction normal or the direction tangential to the contact surface.

The normal force in work reported in the next section was chosen to mimic an elastic-plastic solid (Walton 1993), in which the force is approximated as linear for both loading and unloading. The tangential force is a simplified version of the force proposed by Mindlin (1949), in which the force increases linearly until the Coloumb limit. An analysis of the parametric sensitivity of PD models is given by Cleary et al (1998).

4.3 Heuristic Models

Consider next heuristic models for mixing and segregation fluxes. The ordinary diffusion flux results in mixing caused by concentration gradients and may be written (Bird et al 1960) as

$$j_z^f \;=\; -nD_{coll}\,\frac{df}{dy}, \tag{7}$$

where n is the total number density, f is the number fraction of one of the components, and D_{coll} is the collisional diffusion coefficient. Savage (1993) proposed the following scaling relation for the diffusion coefficient based on hard-particle dynamics simulations:

$$D_{coll} \;=\; f(v)d^2\,\frac{dv_x}{dy}, \tag{8}$$

where $v_x(y)$ is the velocity within the layer, and y is the coordinate normal to the free surface so that dv_x/dy is the velocity gradient across the layer and d is the particle diameter. This expression can be justified on dimensional grounds—similar to those of mixing-length arguments in turbulent flows—assuming that material properties, such as Young moduli, Poisson ratios, etc, play a secondary role. The prefactor $f(v)$ has been determined computationally (Savage 1993) and is a decreasing function of the solids' volume fraction, v, that depends on the value of the restitution coefficients of the particles. Recent computational results of Campbell (1997) show that the diffusion flux is anisotropic; however, the dependence of the diffusivity on the velocity gradient and particle size is as given above.

Savage & Lun (1988) obtained a theoretical estimate of the percolation flux for segregation of a mixture of different-sized particles in a chute flow by using a statistical approach. The analysis was based on the assumption that, in a dense flowing layer, small voids are more likely to be formed than larger ones. Thus, smaller particles drop into voids with a greater frequency, as compared with larger particles, resulting in a larger downward flux of the smaller particles. The reverse flux, which results from the requirement of maintaining a zero total flux of particles normal to the layer, is the same for both types of particles. The net result is a downward flux of the smaller particles and an upward flux of the larger particles, resulting in segregation. The distribution of void sizes was obtained by considering simple arrangements of particles in a layer, and the frequency of dropping was obtained from dimensional analysis. Theoretical predictions were in agreement with experimental results for chute flow of a mixture of particles of different sizes described above.

In the case of equal-sized particles with different densities, the driving force for segregation may be imagined to be the effective "buoyant force" experienced by the particles; lighter particles may be considered to be immersed in an effective medium of higher density corresponding to the average density of the mixture, and heavier particles in a lower-density-effective medium. This idea forms the basis for a heuristic model for the density segregation flux (Khakhar et al 1997b). The merits of this idea can be investigated by means of MC simulations, PD simulations, and theory, and these investigations are discussed below.

Dolgunin et al (1998) have proposed a phenomenological model for the segregation flux due to size and density differences in which one term is similar in

form to that obtained by Khakhar et al (1997b) and a second is of the form of a diffusive flux (Equation 7) but with a negative diffusion coefficient. Predictions of this model were in good agreement with experimental data for chute flow.

Although the theories for segregation reviewed above provide some physical insight into the process and are reasonably successful in describing segregation in chute flows, few are grounded on fundamentals, and even the driving forces for segregation are not clear in many cases. Statistical mechanical studies of hard-sphere mixtures provide a starting point for understanding granular segregation, and we review these next.

4.4 Kinetic-Theory-Based Models

The most complete kinetic theory for multicomponent mixtures of hard spheres is given by de Haro et al (1983). Jenkins & Mancini (1989) showed that the equations derived by de Haro et al (1983) are valid to the first order of approximation for slightly inelastic spheres. Hsiau & Hunt (1996) considered the shear flow of a binary mixture of different-sized particles, using the kinetic-theory results. The gradient in temperature across the layer results in the smaller particles migrating to the higher velocity and thus higher-temperature regions. Extrapolating these results to temperature-induced segregation in a chute flow leads to a prediction that the smaller particles migrate to the top of the layer; this is the reverse of the predictions of Savage & Lun (1988). Gravitational effects were not considered in the study, and these could produce pressure gradients that could reverse the segregation flux as shown in the next section. Kincaid et al (1987) computed thermal diffusion factors (α_{ij}) defined by $\alpha_{ij}\nabla\ln T = \nabla \ln(n_j/n_i)$ to characterize the segregation in mixtures of hard-sphere molecules due to temperature gradients. Here n_i is the number density of species i and T is the temperature, and the thermal diffusion factor gives the magnitude and direction of the segregation relative to the temperature gradient. Arnarson and Willits (1998) computed the thermal diffusion factors defined above for binary mixtures of slightly inelastic particles taking into account both granular temperature and pressure gradients in one spatial direction. Computational results are presented to map out regions of the parameter space (size ratio, density ratio, solids volume fraction, number fraction, and the ratio of the pressure gradient normalized by the number density to the temperature gradient) in which α_{ij} is positive or negative. The kinetic-theory results permit a general understanding of the causes of segregation, and we review these next.

Diffusion may occur due to three independent causes (Hirschfelder et al 1954, Bird et al 1960): ordinary diffusion caused by number fraction gradients, temperature diffusion due to gradients in the granular temperature, and pressure diffusion caused by pressure gradients. Ordinary diffusion always results in mixing, whereas pressure and temperature diffusion produce segregation if there exist density and size differences. Expressions for the different diffusion fluxes from the kinetic theory for binary mixtures are given by Khakhar et al (1999b). The

coefficients of diffusion for the three driving forces depend on the chemical potential of each of the species and have a complicated form. In the limit of low-volume fractions, however, they reduce to the simple forms obtained for ideal hard-sphere gases (Hirschfelder et al 1954), and these are given below.

Consider a binary system consisting of particles with masses m_1 and m_2. The ordinary diffusion flux obtained from the theory is

$$\mathbf{j}_1^f = -\frac{D_{12}m_1m_2n^2}{\rho}\,\nabla f, \tag{9}$$

the pressure diffusion flux is

$$\mathbf{j}_1^p = \frac{D_{12}\rho_1\rho_2}{\rho^2 T}\,(m_1 - m_2)\nabla p, \tag{10}$$

and the temperature diffusion flux is

$$\mathbf{j}_1^T = -\frac{D_{12}\rho_1\rho_2 n^2}{\rho^2}\,K_T\,(m_1 - m_2)\,\nabla\,\ln T. \tag{11}$$

In the above equations, $\rho_i = n_i m_i$, $i = 1,2$ are mass densities, where n_i, $i = 1$, 2 are the number densities of the two components, $f = n_1/n$, is the number density of component 1, $\rho = (\rho_1 + \rho_2)$ is the total mass density, D_{12} is the binary diffusion coefficient, and K_T the thermal diffusion coefficient. The flux equations show that differences in the particle masses result in segregation if a pressure or a temperature gradient exists; however, gradients in concentration result in mixing because the ordinary diffusion flux acts to reduce concentration gradients. Further, if we assume $m_1 > m_2$, the equations show that the particles with larger masses move to regions of higher pressure (owing to pressure diffusion) and into regions of lower temperature (owing to temperature diffusion). Segregation is independent of the sizes of the particles in this case.

The equations for the pressure and ordinary diffusion fluxes for equal-sized particles with different densities are identical to the corresponding equations for an ideal gas given above (Khakhar et al 1999b); the form of the binary diffusivity, however, is different. The temperature diffusion flux does not contribute to segregation in this case. Thus, denser particles always concentrate in regions of higher pressure, regardless of the granular temperature profile. The case of different-sized particles with equal density is more complex, and the direction of the segregation flux depends on both the temperature and pressure gradient, as illustrated in the next section for segregation in a flowing layer.

4.5 Equilibrium Segregation in a Flowing Layer

A balance between the diffusion and segregation fluxes results in an equilibrium number fraction distribution in the layer at long times. The pressure gradient in the system is obtained as

$$\frac{dp}{dz} \; = \; - \rho g \; \cos \; \beta, \tag{12}$$

where z is the distance measured normal to the flowing layer, and β is the angle of inclination of the layer.

Consider density segregation of equal-sized particles. Combining Equations 9 and 10, substituting for the pressure gradient by using Equation 12, and integrating, we get (Khakhar et al 1999b)

$$\ln\!\left(\frac{f}{1-f}\right) \; = \; \ln\!\left(\frac{f_0}{1-f_0}\right) \; - \; \frac{(m_1 - m_2)g \; \cos \; \beta}{T} \; (z - z_0), \tag{13}$$

where f_0 is the number fraction at position $z = z_0$. Thus, if the model holds, a plot of $\ln[f/(1 - f)] = \ln(n_1/n_2)$ versus z should produce a straight line. Both MC and PD simulations seem to verify this prediction (Figure 3). In the case of MC ($\beta = 0$), the theory is essentially exact, and there are no fitting parameters; however, for PD simulations the granular temperature is taken to be a fitting parameter. The granular temperature computed from the PD simulations is much lower than the fitted temperature, indicating that the kinetic theory breaks down for large deviations from the assumption of nearly elastic collisions—for PD simulations, friction and collision result in a highly dissipative system. The form of the segregation flux (Equation 9) appears to be valid even for this case.
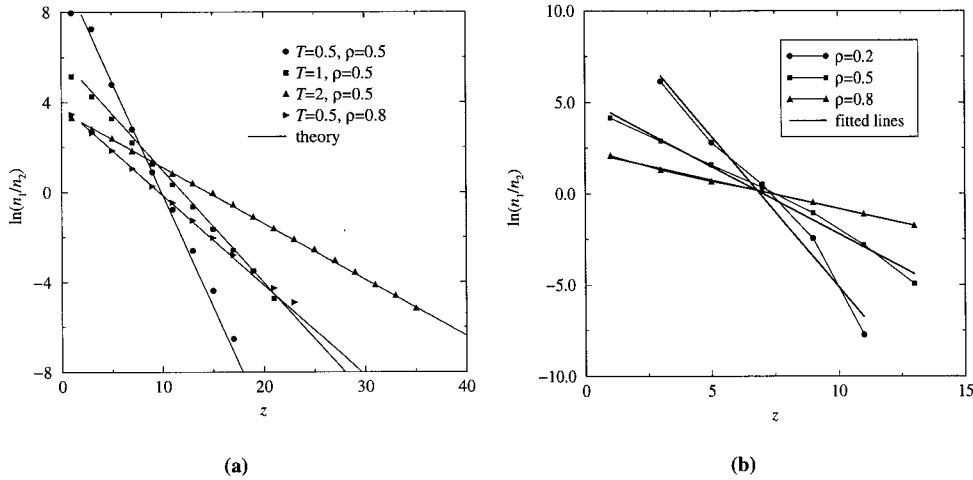

Figure 3 Equilibrium dimensionless number ratio profiles for equal-sized particles with different densities in a layer. (a) Results of Monte Carlo simulations for elastic frictionless particles (*points*) and theoretical predictions of Equation 13 (*lines*). (b) Results of particle dynamics simulations for inelastic, frictional particles in chute flow (*points*) and predictions of Equation 13, using fitted temperature values (*thick lines*) (from Khakhar et al 1999b).

The form of the segregation flux obtained after substituting for the pressure gradient is identical to that obtained from the effective medium arguments for buoyancy-driven segregation discussed above, and consequently the equilibrium profile is also the same (Khakhar et al 1997b). Thus, pressure diffusion in a flowing layer for a mixture of equal-sized, different-density particles essentially results from buoyancy forces.

The predictions of kinetic theory for segregation in a chute flow of a mixture of different-sized particles are shown in Figure 4. In the upper part of the layer, the number ratio (n_1/n_2) decreases with height, implying that the flux of the smaller particles is upwards in the low-volume fraction region. This is expected based on the predictions of Equations 9–11, obtained in the low-volume fraction limit. However, flux reversal and significant segregation occur in the high-volume fraction region; the number ratio sharply increases with distance in this region (Figure 4a). Thus, the existence of a small positive temperature gradient along with a pressure gradient in a high-volume fraction region results in strong reverse segregation, with the smaller particles concentrating in the lower levels. The theoretical predictions agree reasonably well with PD simulations for inelastic, frictionless particles. The volume fraction is uniformly high across the layer in PD simulations with inelastic frictional particles, and, in this case, the smaller particles concentrate only in the lower regions of the layer (Figure 4b). Again the theory gives reasonable predictions of the profiles if an effective temperature
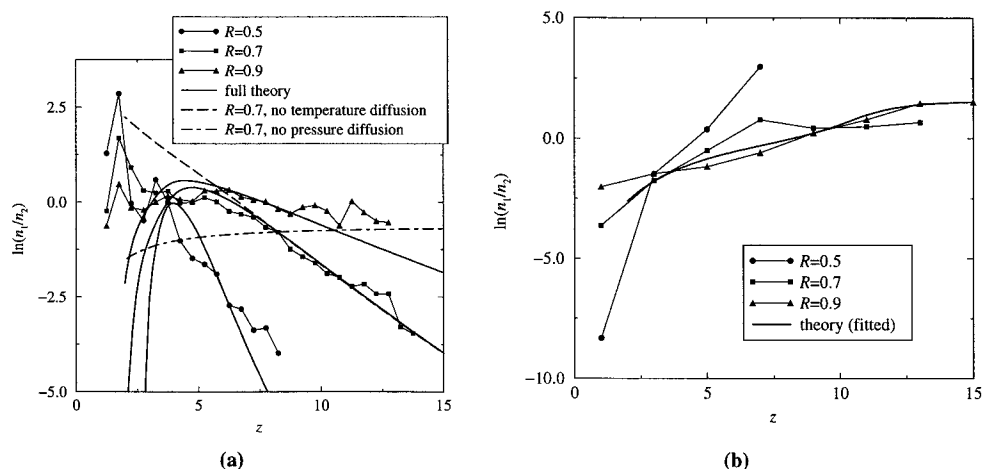

Figure 4 Equilibrium-dimensionless number ratio profiles for different-sized particles with equal densities for chute flow. (a) Results of particle dynamics simulations for inelastic frictionless particles (*points*) and theoretical predictions using kinetic theory (*lines*). (b) Results of particle dynamics simulations for inelastic, frictional particles (*points*) and predictions of kinetic theory with a fitted temperature profile (*thick lines*) (from Khakhar et al 1999b).

profile is used. The results presented here aid in explaining the reversal in pattern of radial segregation observed by Nityanand et al (1986). At low rotational speeds, slow flow in the cascading layer of the rotating drum results in high-solids volume fractions, and thus smaller particles sink to lower parts of the layer, resulting in the formation of a core of the smaller particles. However, at higher speeds, because of the lower-volume fractions in the flowing layer, the smaller particles concentrate in the upper parts of the layer, forming a core of the larger particles with the smaller particles at the periphery.

The above results show the utility of the constitutive equations for diffusion, and these can be incorporated into a general description of mixing and segregation based on advection equations. This issue is considered in Section 8.

5. MIXING BY ROTATION IN CYLINDERS

There has been a considerable amount of work addressing mixing in cylinders. The studies can be broadly classified into the following three categories based on their focus: (*a*) studies of the time evolution of the mixed state, (*b*) studies of axial dispersion, and (*c*) studies of transverse mixing. A few important aspects are reviewed here.

The approach in studies in the first category, time evolution of the mixed state, is to characterize the efficacy of mixers by determining the time evolution of a global mixing index, a statistical measure that reflects the extent of mixing. Indices (several have been proposed; Fan et al 1990) are typically determined by sampling the composition at different (usually random) positions within the mixer. A typical measure of the mixed state is the intensity of segregation (Danckwerts 1952), defined as the standard deviation of the number fraction of the tracer particles from the mean value. A key result common to many such studies is that, initially, the intensity of segregation decays exponentially with time. Significant advances have been made in sampling procedures and analysis of data (Muzzio et al 1997). Although this approach has been useful for determining the effect of system parameters (e.g. baffles, Wes et al 1976) on the rate of mixing in a particular mixer, it gives little insight into fundamental mechanisms of mixing.

In studies of axial dispersion, axial mixing is determined primarily by particle diffusion in the flowing layer and is typically slow (Hogg et al 1966). The mixing is characterized in terms of the axial-dispersion coefficient, the effective diffusion coefficient in the axial direction, and this parameter has been measured for closed rotating cylinders (Hogg et al 1966) as well as rotating cylinders with a continuous flow of solids through them (Hehl et al 1978). The latter is of particular importance for the analysis of rotary kilns. In closed systems, typically half the length of the drum is filled with one component and the other half with the second component, thus producing a step concentration profile at the start of the experiment. The dispersion coefficient is obtained from the concentration profile along the cylinder after sufficient rotation time. The continuous-flow experiments

involve injecting a pulse of the tracer material at the entrance and measuring the exit concentration of the tracer as a function of time. The axial-dispersion coefficient is obtained from the spreading of the pulse. Typical values of the axial-dispersion coefficient in a laboratory scale cylinder ($\sim$8 cm in diameter) are about 10^{-6} m^2/s for particles of average size 200 μm. Studies indicate that the axial dispersion increases with rotational speed of the mixer and particle size (Rao et al 1991).

The issue of transverse mixing in a rotating drum in the continuous-flow regime was first analyzed by Hogg & Fuerstenau (1972) and Inoue et al (1970) using idealized flow models. Particles entering the flowing layer from the bed were assumed to instantly re-enter the bed at the same radial position in the lower half of the layer, in the work by Hogg & Fuerstenau (1972), whereas particles were assumed to enter at a random position in the lower half in Inoue et al (1970). Visualization studies of the mixing with colored tracer particles were carried out by Lehmberg et al (1977), and recently a continuum analysis and experiments for mixing in this regime were presented by Khakhar et al (1997b). Although most studies have focused on the continuum regime, there has been a recent surge of interest in mixing in the avalanching regime (Metcalfe et al 1995, Elperin & Vikhansky 1998b). Geometrical aspects dominate in the avalanching regime, whereas dynamic effects predominantly control mixing in the continuous-flow regime. Transverse mixing in both regimes is considered below.

5.1 Transverse Mixing in the Avalanching Regime

Consider mixing in a quasi–two-dimensional, cylindrical rotating drum partially filled with granular particles (see Section 2). If the rotation speed, ω, is sufficiently slow, the flow is time periodic and consists of distinctly separated avalanches; one avalanche starts and ends before the next one starts and ends and so on. The angle of the free surface (β in Figure 2) grows until a discrete avalanche occurs, and β relaxes from its preavalanche angle, β_i, to a new angle, β_f. These two angles define two wedges, an initial preavalanche wedge and a final, postavalanche wedge. As the avalanche occurs, material in the uphill wedge flows to fill the downhill wedge. Thus the motion can be decomposed into two components: a geometrical component, consisting only of the transport of the wedges, and a dynamical component, consisting of a complex rearrangement of material within the wedge.

Geometrical insight reveals several things about the qualitative behavior of this kind of mixing device. Regardless of the quality of mixing within the wedge, material cannot be transported outside of the wedges during an avalanche. Transport from one wedge to a different wedge can occur only if there are quadrilateral intersections between wedges. Thus, at a fill level of 50%, the quadrilateral intersections disappear, and mixing vanishes. In addition, the quadrilaterals expand as the fill level diminishes, so mixing improves for lower fill levels. Also, fill levels of >50% produce a core in the center of the granular mass. No wedges penetrate

the core, so no mixing should occur there. All of these predictions are validated by experiments (Metcalfe et al 1995, see Figure 5*a*). We can use this model to make quantitative predictions as well. The simplest way to do this is to assume that particles within a wedge are completely randomized after each avalanche. Computationally this may be accomplished, for example, by interchanging every particle within the final wedge with another particle, also within the final wedge, chosen at random. Figure 5*b* shows the mixing rates calculated for this problem by this method. As predicted, the mixing rate goes to zero for half-full drums and increases as the fill level is reduced. The results are remarkably insensitive to the precise value of the wedge's angle and, clearly, to the details of mixing within the wedge itself.

The wedge concept can be extended in a variety of ways (McCarthy et al 1996, Ottino & Shinbrot 1999). New issues appear when the containers are concave or when there are baffles. For rotationally symmetric containers, but not reflexionally symmetric ones, experiments and the wedge theory show that containers mix differently depending on the sense of rotation. When the containers have baffles, the theory indicates that symmetrically placed baffles produce no net effect but asymmetrically placed baffles improve mixing. Extensions to three dimensions are also possible; in this case avalanches in two different directions may be combined to produce mixing in the radial and axial directions of a cylinder (McCarthy et al 1996). Much more is possible in this area.

The geometric viewpoint described for the drum mixer survives even if particles are changed, provided that they are not so cohesive that distinct angles of repose become ill defined. For example, the geometrical model works for mixtures of dissimilar particles, such as large round sugar beads and small cubic salt grains. The large unmixed core remains, although the details of mixing in the periphery and in the core may differ significantly from the case of identical powders (Figure 6).

5.2 Transverse Mixing in the Continuous-Flow Regime

We next consider the flow achieved at higher accelerations, the so-called continuous-flow or rolling regime (Figure 2). The process of mixing is very different than that in the avalanching case. Consider an initialized "blob" of particles in the flowing layer; the blob is deformed into a filament by the shear flow and blurred by collisional diffusion until particles exit the layer. Particles then execute a solid-body rotation in the bed and reenter the layer, and the process repeats. For the cylinder and if the composition of the particles in the layer does not change (in particular, if all the particles are identical), the mean flow is time independent, and the streamlines (lines tangent to the mean-velocity field) act as impenetrable barriers to convective mixing.

Figure 7 shows the time evolution of tracer particles during a typical mixing experiment. The mixing process can be simulated by solving the convective diffusion equation for the tracer concentration, using the flow discussed in Section
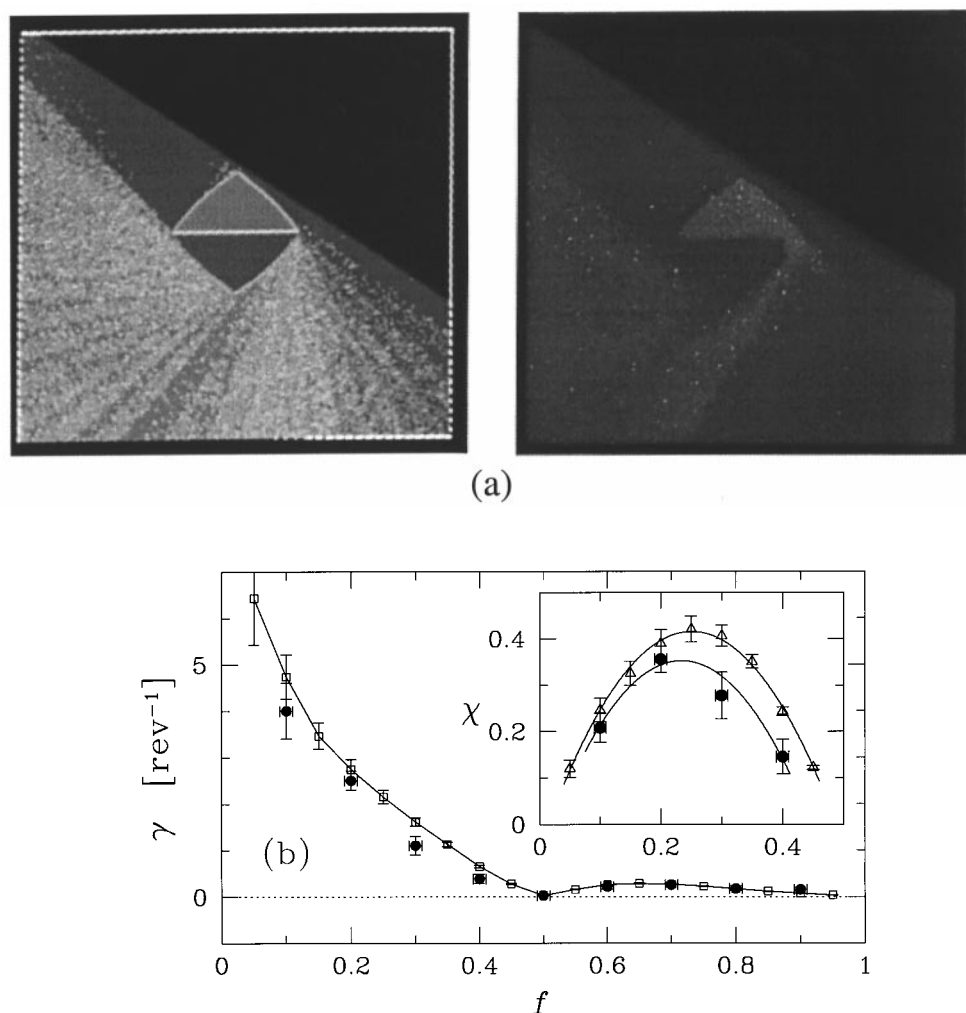
Figure 5 Granular mixing of different colored but otherwise identical particles in the avalanching regime. (a) Comparison of simulation (*left*) with experiment (*right*) in a square mixer. (b) Variation of the mixing-rate exponent (γ) with fractional filling (f) for a circular mixer. The location of the centroid of the particles of one type (e.g. *light colored*) approaches the centerline at an exponential rate with an exponent γ. The *symbols* are experimental results, and the *lines* are predictions of the model. The *inset* shows variations of volumetric mixing rates ($\chi = \gamma V$, where V is the normalized volume of particles being mixed) with the fractional filling f (from Metcalfe et al 1995, reproduced with permission).
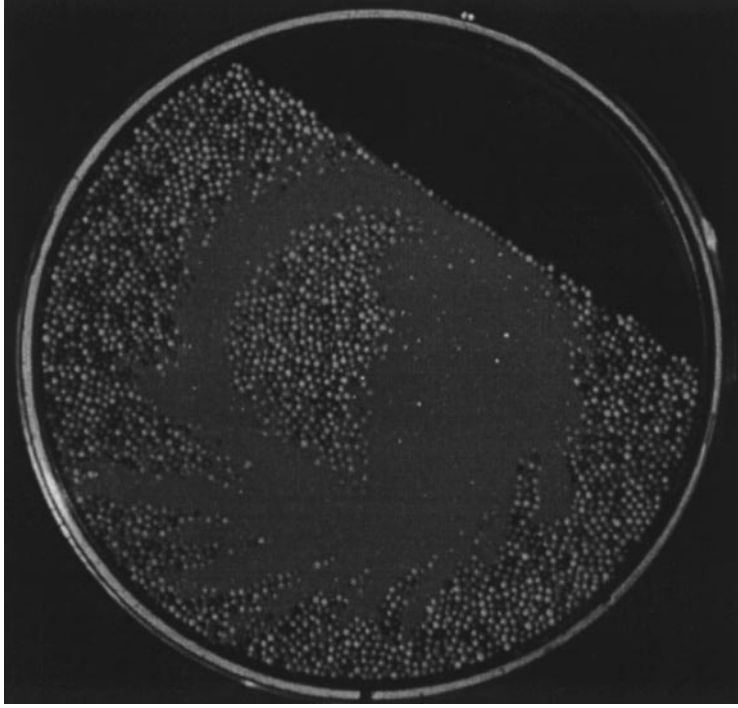
Figure 6 Result of mixing small, dense, cubic particles with large, light, spherical particles in the avalanching regime. Mixing within wedges is dramatically different from that in Figure 5; however, a geometrical core is clearly apparent. The mixing structure outside the core, owing to mixing within the wedges, is radically different (from McCarthy et al 1996, reproduced with permission).

2, Equations 3–5, and the heuristic model for the diffusion. Taking a Lagrangian approach, the motion of tracer particles in the layer (in a continuum sense) is given by

$$\frac{dx}{dt} \ = \ v_x \tag{14}$$

$$\frac{dy}{dt} \ = \ v_y \ + \ S, \tag{15}$$

where S is a white-noise term that, on integration over a time interval (Δt), gives a Gaussian random number with variance $2D_{coll}\Delta t$. Diffusion along the layer (x-direction) is neglected, because diffusional effects are masked by convection [the Péclet number for diffusion in the x direction is $Pe \ = \ uL/D_{coll} \gg 1$, whereas that
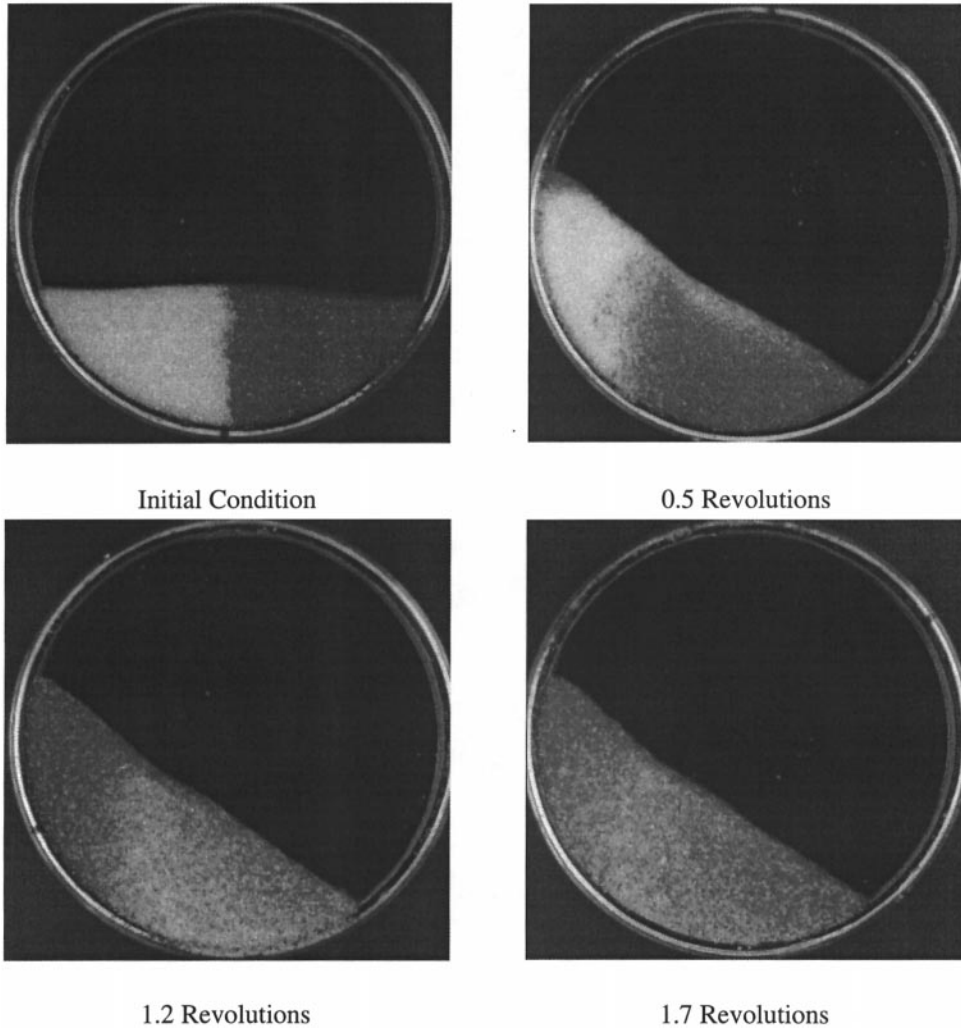
Figure 7 Typical time evolution of mixing of identical particles in the continuous flow regime. Differently colored sugar crystals are mixed at 6 rpm in a cylinder of diameter 14 cm (from Khakhar et al 1997b, reproduced with permission).

in the y direction is smaller by a factor $(\delta_0/L)^2$]. Predictions of the model are in good qualitative agreement with experimental results.

The intensity of segregation (Danckwerts 1952), obtained by image analysis from the experiments and from computations, decays exponentially as

$\exp(-2\pi kN)$, where N is the number of revolutions and k is a constant. The mixing-rate constants obtained from theory and experiment are in reasonable agreement. The data also show the importance of the depth of filling—mixing is very slow for a half-full mixer, although the reasons for this are quite different from those for the avalanching case. Bed depths less than half full result in circulation times that increase with radial distance in the bed, in contrast to the half-full case, in which the circulation times are nearly independent of radius. The less than half-full case leads to an effective shearing between adjacent layers. Reducing the bed depth also reduces the average circulation time for the particles—particles go around more than once in half a revolution of the cylinder. Both of these effects contribute to faster mixing due to smaller bed depths. Higher diffusivities produce faster mixing, as expected.

The computation of the mixing rate reveals that mixing occurs nearly an order of magnitude more slowly in the continuous case than in the discrete, avalanching case; it takes more rotations to achieve the same mixing in the continuous-flow regime. By this measure the discrete avalanching mechanism is more efficient for mixing than the steady, continuous-flow mechanism.

6. TUMBLING AND SEGREGATION

We now consider mixing and segregation in the continuous-flow regime. The case considered corresponds to a binary system, labeled 1 and 2, with particles of the same size but different densities. We assume first that the mean flow is still the same as if all particles were identical. The effects of segregation, as well as those of collisional diffusivity, are important only in the direction normal to the flow, the effects in the x-direction being negligible compared with those of the convective flow as diffusion alone, discussed above. The system is represented by Equations 14 and 15 with the effects of segregation incorporated in Equation 15 in terms of a segregation velocity. The segregation velocity for denser particles is obtained from the segregation flux as

$$v_{y1} = j_{j1}^p/n_1 = \frac{-\gamma_s D_{coll}(1 - \bar{\rho})(1 - f)}{L} \tag{16a}$$

and for the less dense particles as

$$v_{y2} = \frac{\gamma_s D_{coll}(1 - \bar{\rho})f}{L}, \tag{16b}$$

where $\bar{\rho} = \rho_2/\rho_1$ is the density ratio and γ_s, the dimensionless segregation velocity, is taken to be a fitting parameter. Similar expressions can be obtained from Equations 9–11 for systems differing in size, at low-solids volume fractions.

The expressions for high-volume fractions are more complex (Khakhar et al 1999b).

The equilibrium distribution of a segregated mixture of particles with different densities for two extents of filling and different overall particle concentrations is shown in Figure 8. In a cylinder the equilibrium isoconcentration profiles coincide with the streamlines. The concentration of particles depends only on the radial distance, quantified by a surface coordinate x (see Figure 2). Comparison of the theory to the experimental data requires an estimation of only two parameters, D_{coll} and γ_s. It is, however, hard to obtain reliable independent estimates of these quantities. The diffusivity may be estimated from Equation 8, and γ_s can be obtained by performing experiments at one speed and then using this value to fit the rest. The agreement is satisfactory; in fact, it is somewhat surprising to find
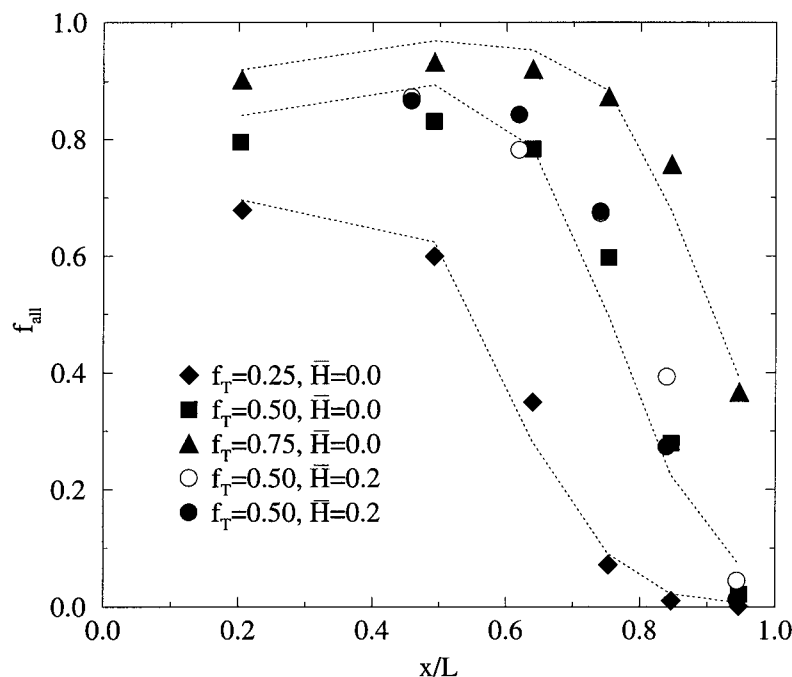

Figure 8 Equilibrium segregation of equal-sized particles with different densities in a circular mixer operating in the continuous-flow regime. The variation of the number fraction of the denser particles in the bed (f_{all}) with distance along the free surface [x/L (see Figure 2)] is shown. *Points* are experimental results for steel balls and glass-bead mixtures with different number fractions of steel balls (f_T) and extents of filling [$\bar{H} = (R - h)/L$, where h is the bed depth, and R is the mixer radius]. The *dashed lines* are model predictions using same fitted values of γ_s and D_{coll} for all three curves (from Khakhar et al 1997b; reproduced with permission).

such good agreement between a continuum theory and experiments, considering that the layer thickness is just 5–6 particle diameters.

The extent of segregation increases with an increase in the dimensionless segregation velocity and dimensionless diffusivity. Simulations demonstrate the competition between segregation and mixing. For slow mixing, the intensity of segregation monotonically decreases to an equilibrium value; for fast mixing, however, there may exist an optimal mixing time at which the best mixing is obtained.

7. CHAOTIC ADVECTION

Chaotic advection, which has been central in advancing fundamental understanding of liquid mixing (Aref 1990, Ottino 1989), is also present in granular flows. Consider the mixing of similar cohesionless powders, when segregation effects are unimportant (Khakhar et al 1999a). If the cross section of the rotating container is circular, the mean flow is time independent, and the streamlines (lines tangent to the mean-velocity field) act as impenetrable barriers to convective mixing. Mixing theory shows that time modulation of streamlines is generally sufficient to produce chaotic advection (Ottino 1990). In a rotating tumbler, chaotic advection simply happens when the cross-section is not circular.

Chaotic systems display regular (nonchaotic) and chaotic regions. The stretching in chaotic regions is exponential (good mixing), whereas in regular regions it is linear (poor mixing). The standard visualization technique is the Poincaré section a mapping of the position of selected particles (in the continuum sense) after each half rotation of the mixed. To adapt the model of Equations 3–5 to noncircular mixers, one needs only change the form of L, now a function of time. For example, for an elliptical mixer, the length of the flowing layer $L(t)$ is given by

$$L(t) = \frac{ab}{[b^2 \cos(\omega t + \alpha) + a^2 \sin(\omega t + \alpha)]^{1/2}}, \qquad (17b)$$

where a and b are the major and minor semiaxes of the ellipse, respectively, and α is the initial (at $t = 0$) angle between the free surface and the major axis of the ellipse. The layer thickness and length change slowly with mixer rotation, but the layer geometry remains similar at all orientations, the ratio δ_0/L being constant. Figure 9 (see color insert) shows the Poincaré sections for a half-filled ellipse (Figure 9b) and square (Figure 9c), respectively, illustrating regions where particles can be trapped near elliptic points (marked in red) and regions where chaotic trajectories exist near hyperbolic points (marked in blue). To isolate the effects of advection, the collisional diffusivity is set equal to zero. The length stretch in the chaotic mixers is exponential, whereas it is linear in the circular mixer (nonchaotic).

Figure 10 (see color insert) shows a comparison between computations and experiments in square containers. In this case, collisional particle diffusion is assumed in the model ($D_{coll} = 10^{-3}$ m²/s). A quantitative comparison of the evolution of mixing with time is given in Figure 11 in terms of the intensity of segregation (Danckwerts 1952), which is essentially the standard deviation of the concentration of the tracer particles. These results indicate that the theory describes the mixing process in both qualitative and quantitative terms.

Collisional diffusion plays an important role in chaotically advected systems. The effects are scale dependent. The relative importance of advection to diffusion can be estimated in terms of the Péclet number: the ratio of diffusion time, δ_0^2/D_{coll}, to advection time, u/L; that is,

$$Pe = \frac{\delta_0^2 u}{L D_{coll}}. \tag{18}$$

Using the result $\delta_0 = kL$, and setting $f(\nu) = 0.025$ in Equation 4, we obtain

$$Pe = 20k^3 \left(\frac{L}{d}\right)^2. \tag{19}$$

Thus the effectiveness of diffusion decreases with increasing system size relative
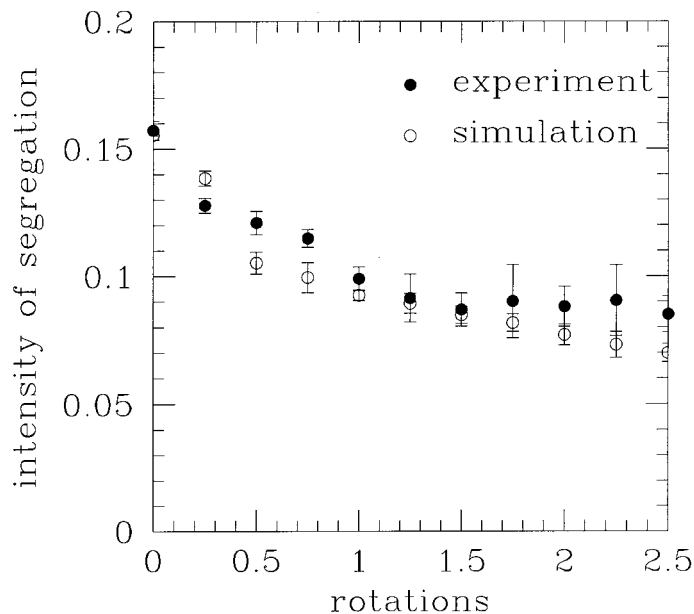

Figure 11   Variation of the intensity of segregation versus mixer rotation corresponding to the experimental and theoretical results of Figure 10. The *filled circles* represent experimental values, and the open *circles* denote values obtained from the model (from Khakhar et al 1999a, reproduced with permission).

to particle size, and collisional diffusion plays a minimal role in large scale systems. Figure 12 shows a comparison of the rate of evolution of the mixing in terms of the intensity of segregation for chaotic and nonchaotic systems for two different mixer sizes. As may be expected, collisional diffusion plays a more central role in nonchaotic systems. The mixing is much faster in the chaotic system.

8. CHAOS AND SEGREGATION

Segregation and advection interact in unexpected ways. Consider the experimental evidence first. Equilibrium segregation structures for half-filled mixers are shown in Figure 13 for systems of spheres differing in density (Figure 13*a–c*) and size (Figure 13*d–f*). The mixtures consist of 75% 2-mm-diameter steel beads by volume and 25% of either 0.8-mm glass beads or 2-mm steel beads. Similar results are obtained for mixtures ranging from 25% to 75% 2-mm steel beads.
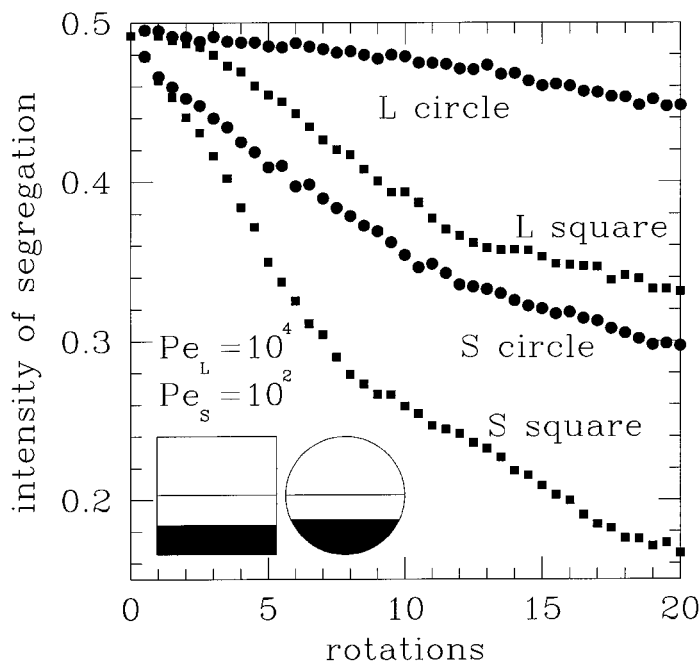

Figure 12 Variation of the intensity of segregation versus mixer rotation obtained for mixers of different shapes and sizes by computations. The large systems correspond to a Péclet number $Pe = 10^4$, and the small systems correspond to $Pe = 10^2$, which indicates, everything else being equal, a mixer size ratio of 10 (from Khakhar et al 1999a, reproduced with permission).

However, the clearest illustrations correspond to a lower fraction of the smaller (or denser) spheres.

The classic segregated structure for the circular mixers—the radial segregation pattern (shown in Figures 13a, d)—leads to a segregated time-invariant core region that coincides with the streamlines. The equilibrium segregation structures in noncircular mixers are radically different. This is perhaps most dramatic for a half-filled square mixer (Figures 13c, f), where the segregated core is located away from the center of rotation and is nearly separated into two regions between the corners of the square and the center of rotation. The corresponding segregation structure for the ellipse shows, like the square, that the smaller (denser) particles are pulled away from the center of rotation. The segregated region (or regions, depending on the instantaneous orientation) form a pattern that is periodic in time.

Incorporating the density segregation flux [equations (16a) and (16b)] into the flow model for non-circular mixers, discussed in the previous section, allows the calculation of the equilibrium segregated patterns (Figure 13h, i). The computed patterns are in good agreement with those obtained experimentally for systems with equal-sized particles with different density (Figure 13a, b).

An assumption of the model is that the flow in the layer is independent of particle concentration of the heavier particles. Although this is reasonable for equal-sized particles with different density, it is a bad assumption for particles of different sizes; experiments (Hill et al 1999a) and theory (Jenkins & Mancini 1989) show that flows may become much faster on the addition of small particles. Comparison of the experimental structures with the corresponding Poincaré sections (Figure 9b, c) reveals that the equilibrium segregation patterns strongly resemble the underlying Poincaré sections. The segregated regions are similar (but not identical) to the regular islands in the Poincaré sections; for example, there is some asymmetry of the segregated structures that is especially apparent for the ellipse. Kolmogorov-Arnold-Moser islands displayed in Poincaré sections are invariant regions of the single component flow, that is, when there is no segregation (islands, in general, deform; i.e. the exact details of the Poincaré section depend on the instantaneous orientation of the mixer). In case an island contains only heavier particles ($f \approx 1$) we have $v_{y1} = 0$ [equation (16a)], so that the flow field for the particles in the island is identical to that for a single component system. Thus heavier particles that sink into islands are likely to be mapped back to the same region. Heavy particles outside the islands are mixed by chaotic advection and diffusion.

There are also some discrepancies between the Poincaré sections and the equilibrium segregation patterns. For example, there is asymmetry in the segregation patterns that are not present in the Poincaré section; this is most obvious in the ellipse. The Poincaré sections are computed for a system of identical particles (i.e. a continuum description of the granular flow). The trajectory of the heavier particles deviates from this "base case," owing to their segregation velocity, and this deviation is always downward and backwards in the flowing layer: this leads to the asymmetry observed experimentally. Asymmetric structures are obtained in the computations as well (Figures 13h, i see color insert).

Additional similarities are found between the Poincaré sections and the segregation patterns when the mixers are no longer half filled. Both the Poincaré section and the equilibrium segregation structures depend strongly on the degree of filling at about the half-full level.

The above discussion can be extended to mixtures of particles that differ in size. The similarity with the underlying Poincaré section holds (within bounds). There are important additional physical effects, however; unlike identical or equal-sized particles, the flow in the layer of different-sized particles changes (noticeably) depending on the particles present. If the flowing layer consists entirely of small particles, it is thinner and moves faster; conversely larger particles form a deeper and more slowly flowing layer. Thus, the velocity field is now coupled to the composition of the particles in the layer, and this leads to new effects.

An example of the complexity introduced by the coupling between velocity and concentration is the radial streak structure shown in Figure 14a (see color insert). This instability resembles that in the formation of a two-dimensional heap (Maske et al 1997) and is particularly apparent for mixers that are filled just above the half-full level. In this case, each entire stripe enters the flowing layer all at once, and the instability is reinforced. This phenomenon appears to be independent of the underlying Poincaré section (it occurs in mixers of all shapes). A description of this result is given by Hill et al (1999a). Increasing the degree of filling results in a radically different structure (Figure 14b).

9. ROLE OF COHESION

This review has so far considered only noncohesive systems; the only interparticle forces in these systems occur when particles touch each other. This is a good assumption for systems with large dry particles, for example, >100 μm. Granular materials with smaller-diameter particles, for example in the range <5–10 μm or smaller, are typically cohesive. There has been much interest in cohesive powders in the last few years (Hornbaker et al 1997, Albert et al 1997, Abdel-Ghani et al 1991, Thornton et al 1996, Pierrat & Caram 1997, Bocquet et al 1998). Interparticle forces may be caused by surface adhesion, van der Waals attractive forces, or interstitial forces arising from liquid bridges in wet powders. The issue of liquid bridging between particles appears to have been first considered by Fisher (1926) and more recently by Lian et al (1993, 1998). There is, however, remarkably little work addressing the effects of cohesiveness on mixing.

In principle, cohesion forces can be easily incorporated into particle dynamics simulations. Here we consider briefly the role of liquid bridges in terms of a simple model (McCarthy & Ottino 1998). This is an admittedly difficult case, because, in addition to the capillary force, wet particles are also subject to viscous resistive forces as particles move past each other, multiple interactions are possible, film thicknesses need not be the same in all particles, etc [viscous forces

can be calculated by using lubrication theory; a reference treating this case is Adams & Edmonson (1987)]. An important additional consideration is the surface roughness or asperity of particles. For perfectly smooth particles, lubrication forces become unbounded as the distance between particles goes to zero. In practice, however, surface roughness controls the process at small scales.

The importance of cohesion arising from liquid bridges can be quantified in terms of the Bond number, defined as the ratio of the force caused by interfacial tension and liquid bridging to the weight of the particles,

$$Bo = \frac{2\pi a\gamma}{4\pi a^3 \; \rho g/3}. \qquad (20)$$

Here a is the radius of the particles, and γ the interfacial tension. Note that the adhesion force is proportional to γa regardless of the size of the liquid bridge. This difficulty disappears if roughness is taken into account (Bocquet et al 1998). Obviously, owing to a distribution of liquid among particles, the local value of the Bond (Bo) number may be different from the average value.

The most interesting results are those that present different qualitative aspects than those anticipated based on the noncohesive case. Consider as an example the results shown in Figure 15, corresponding to the continuous-flow regime and $Fr = 0.1$. The mixing rate—as measured in terms of the intensity of segregation— is not monotonic with Bo number: Mixing at moderate Bo is faster than at small Bo, a result that on first viewing appears counter-intuitive. This suggests that there exists an optimal Bo number for mixing in the continuous flow regime.

A recent paper addressing the issue of cohesiveness is Shinbrot et al (1999). Small particle systems behave differently than systems with noncohesive particles. In fact, these authors find that even in the case of a cylinder—due to stick-and-slip motion—that the motion may be chaotic. This has the consequence that small particle systems—i.e. cohesive systems—mix better than noncohesive systems. This is the same conclusion as that of McCarthy & Ottino (1998) though due to a completely different reason. This indicates the richness of this topic.

10. SCALE UP AND LESSONS FOR INDUSTRIAL PRACTICE

What is the status of applied work? How have recent developments in modeling of granular materials been applied to systems of practical interest?

The status of use-inspired work is represented in the reviews of Bridgwater (1976) and Williams (1976) and the more recent ones of Poux et al (1991) and Fan et al (1990). Actual industrial applications, however, rely heavily on experience distilled into experimentally based heuristics guiding mixer selection and scale-up rules (Poux et al 1991, Fan et al 1990). For example, rotating drums are recommended for mixing free-flowing materials with very similar properties,
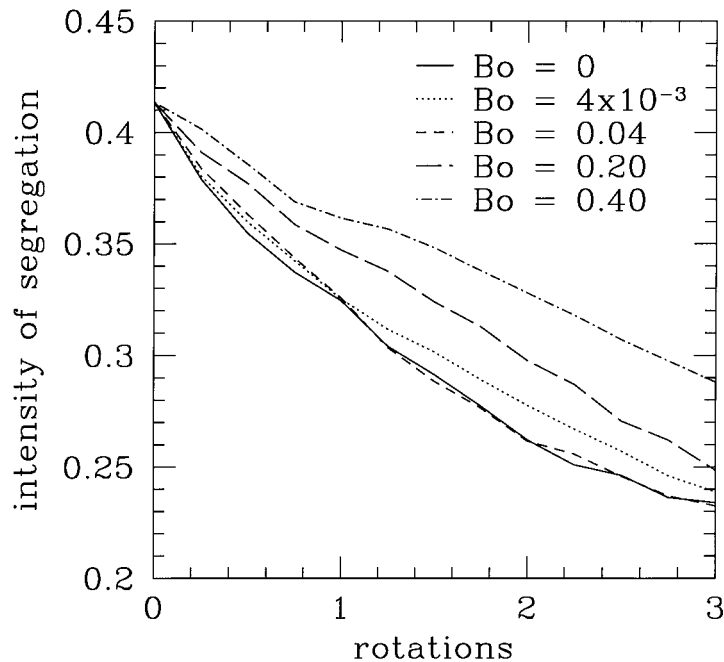
Figure 15 Variation of intensity of segregation with time for mixing of cohesive particles in the continuous-flow regime. Cohesion results from liquid bridging; results for different Bond numbers (see Equation 20 for definition) are shown.

whereas high-shear impellers may be necessary for mixing a very small concentration of one component in another with high uniformity (Poux et al 1991). Loading and cleaning are also important considerations in the choice of mixer, because segregation might occur during unloading (Poux et al 1991, Johanson 1978). For tumbling mixers, scale up is based primarily on equating Froude numbers, although correlations are available to account for particle size during scale up (Fan et al 1990).

Segregation is an important problem, and heuristic rules are typically used to minimize its effects. These rules relate to the type of mixers to be used, the use of additives, and particle properties (Poux et al 1991, Johanson 1978). For example, particle size may have an important effect: particles larger than 70–80 μm segregate readily, whereas particles smaller than 10 μm show little segregation (Nienow et al 1985).

Application of fundamentals for the analysis of mixing has been limited primarily to modeling diffusional mixing in terms of the axial dispersion coefficient (Bridgwater 1976, Fan et al 1990). Geometrical ideas have been used in a recent analysis of mixing of identical particles in a V-blender (Brone et al 1998)—a tumbling mixer made by joining two cylinders at an angle to each other to form

the two arms of a V shape. The mixer is rotated about an axis that intersects both axes of the cylinders, with the three axes forming an A shape. During rotation, when the V is inverted, the material is divided equally into the two arms, and, when the V is upright, the material is in the region of intersection of the cylinders. A simple model in which a fixed mass q (a fitting parameter in the model) is interchanged between the two arms in each rotation gives good agreement with experimental results.

Several fundamental studies have shown that axial mixing (mixing along the axis of rotation) in tumbling mixers is typically slow, because it is determined to a large extent by diffusive motion of the particles. Recent studies have shown how mixing identical particles can be significantly accelerated by rocking the axis of rotation in a vertical plane for rotating drums (Wightman & Muzzio 1998a) and V-blenders (Brone et al 1997). The results also appear to be valid for segregating systems (Wightman & Muzzio 1998b). This represents a nice example of how fundamental insights can lead to improved mixing practices for granular materials. Clearly, much remains to be done in the area of design and scale up of industrial mixers.

11. CONCLUSIONS

The foregoing review organizes concepts in mixing and segregation; it is hoped that the structure serves to highlight critical areas and voids in coverage. The areas of opportunity are many. As we have seen, the container's shape and the degree of filling have a profound effect on mixing, depending on the regime. The avalanching regime leads to unmixed cores; noncircular containers lead to chaotic advection. However, this represents only the beginning, for the containers considered are a small class of possible shapes. All shapes explored so far are rotationally symmetric; they are regular polygons in the avalanching-wedge model; the continuous-flow model applies best to half-filled convex containers, which are symmetric with respect to 180° rotations about their centroids. Geometrical aspects need to be investigated further for the avalanching regime; for example, nonregular shapes, and models for the continuous flow regime need to be refined to account for up and down motion of the shear layer itself.

The segregation models consider only limits. In a segregation plane with axis ρ_1/ρ_2 and d_1/d_2, we consider only the cases in which $\rho_1/\rho_2 \neq 1$, $d_1/d_2 = 1$ and $\rho_1/\rho_2 = 1$, $d_1/d_2 \neq 1$; models for combined size and density segregation remain to be developed. An even more complicated issue is particle shape—methods for characterization of shapes are not well established, and this is particularly important for irregularly shaped particles (Meloy et al 1986); particle shapes and surface roughness are important parameters, in addition to size and density, that influence flow and segregation. It is apparent that the treatment of cohesiveness is only in its infancy and much remains to be done. Moreover, we have not addressed the issue of combined cohesion and segregation and in what ways they may compete

with each other. Finally an even more complex situation is the interplay between segregation, cohesiveness, and chaos in noncircular containers.

Granular materials produce striking structures. The visual display of the competition between chaos-enhanced mixing and property-induced demixing goes beyond granular materials, however; the patterns are striking examples of how simplicity and complexity coexist (Goldenfeld & Kadanoff 1999). In fact, it may be argued that these mixing/demixing systems are simpler—from an experimental viewpoint (Hill et al 1999b)—than systems undergoing spinodal decomposition (Onuki 1997, Wagner & Yeomans 1998) or diffusion-reaction patterns in chemical reactions (Epstein & Showalter 1996). It is hoped that, when taken as a whole, these developments will open the mixing arts to first-principles analysis and successful modeling.

ACKNOWLEDGMENTS

Visit the Annual Reviews home page at www.AnnualReviews.org.

LITERATURE CITED

Abdel-Ghani M, Petrie JG, Seville JPK, Clift R. 1991. Mechanical properties of cohesive particulate solids. *Powder Technol.* 65: 113–23

Adams MJ, Edmonson B. 1987. Forces between particles in continuous and discrete fluid media. In *Tribology in Particulate Technology,* ed. BJ Briscoe, MJ Adams, pp. 154–72. Philadelphia: Adam Hilger

Albert R, Albert I, Hornbaker D, Schiffer P, Barabasi A-L. 1997. The angle of repose in wet and dry granular media. *Phys. Rev. E* 56:R6371–76

Allen MP, Tildesley DJ. 1987. *Computer Simulation of Liquids.* Oxford, UK: Oxford Univ.

Alonzos M, Satoh M, Miyanami K. 1991. Optimum combination of size ratio, density ratio and concentration to minimize free surface segregation. *Powder Technol.* 68:145–52

Aref H. 1990. Chaotic advection of fluid particles. *Philos. Trans. R. Soc. London Ser. A* 333:273–88

Arnarson BÖ, Willits JT. 1998. Thermal diffusion in binary mixtures of smooth, nearly elastic spheres with and without gravity. *Phys. Fluids* 10:1324–1328

Bagnold RA. 1954. Experiments on a gravity-free dispersion of large solid spheres in a Newtonian fluid under shear. *Proc. R. Soc. London Ser. A* 255:49–63

Baumann G, Janosi IM, Wolf DE. 1995. Surface properties and flow of granular material in a two dimensional rotating drum, *Phys. Rev. E* 51:1879–88

Bird RB, Stewart WE, Lightfoot EN. 1960. *Transport phenomena.* New York: Wiley & Sons 780 pp.

Bocquet L, Charlaix E, Ciliberto S, Crassous J. 1998. Moisture-induced aging in granular media and the kinetics of capillary condensation. *Nature* 396:735–37

Boutreux T, de Gennes PG. 1996. Surface flows of granular mixtures. I. General principles and minimal model. *J. Phys. I, France* 6:1295–304

Bridgwater J. 1976. Fundamental powder mixing mechanisms. *Powder Technol.* 15:215–36

Bridgewater J. 1995. Particle technology. *Chem. Eng. Sci.* 50:4081–89

Bridgwater J, Cooke MH, Scott AM. 1978. Interparticle percolation: equipment development and mean percolation velocities. *Trans. Inst. Chem. Eng.* 56:157–67

Bridgwater J, Foo WS, Stephens DJ. 1985. Particle mixing and segregation in failure zones—theory and experiment. *Powder Technol.* 41:147–58

Brone D, Alexander A, Muzzio FJ. 1998. Quantitative characterization of mixing of dry powders in V-blenders, *AIChE J.* 44:271–78

Brone D, Wightman C, Connor K, Alexander A, Muzzio FJ, Robinson P. 1997. Using flow perturbations to enhance mixing of dry powders in V-blenders. *Powder Technol.* 91:165–72

Campbell CS. 1997. Self-diffusion in granular shear flows. *J. Fluid Mech.* 348:85–101

Cantalaube F, Bideau D. 1995. Radial segregation in a 2D drum: experimental analysis. *Europhys. Lett.* 30:133–38

Choo K, Molteno TCA, Morris SW. 1997. Travelling granular segregation patterns in a long drum mixer. *Phys. Rev. Lett.* 79:4994–97

Cleary PW, Metcalfe G, Liffman K. 1998. How well do discrete element granular flow models capture the essentials of mixing processes? *Appl. Math. Model.* 22:995–1008

Clément E, Rajchenbach J, Duran J. 1995. Mixing of a granular material in a bidimensional rotating drum. *Europhys. Lett.* 30:7–12

Cooke MH, Bridgwater J. 1979. Interparticle percolation: a statistical mechanical interpretation. *I&EC Fundam.* 18:25–27

Cundall PA, Strack DL. 1979. A discrete numerical model for granular assemblies. *Géotechnique* 29:47–65

Danckwerts PV. 1952. The definition and measurement of some characteristics of mixtures. *Appl. Sci. Res.* A 3:279–96

Das Gupta S, Bhatia SK, Khakhar DV. 1991. Axial segregation of particles in a horizontal rotating cylinder. *Chem. Eng. Sci.* 46:1513–17

de Haro ML, Cohen EGD, Kincaid JM. 1983. The Enskog theory for multicomponent mixtures. I. Linear transport theory. *J. Chem. Phys.* 78:2746–59

Dolgunin VN, Kudy AN, Ukolov AA. 1998. Development of the model of segregation of particles undergoing granular flow down an inclined plane. *Powder Technol.* 96:211–18

Dolgunin VN, Ukolov AA. 1995. Segregation modelling of particle rapid gravity flow. *Powder Technol.* 83:95–103

Donald MB, Roseman B. 1962. Mixing and demixing of solid particles. Part 1. Mechanisms in a horizontal drum mixer. *Br. Chem. Eng.* 7:749–52

Drahun JA, Bridgwater J. 1983. The mechanics of free surface segregation. *Powder Technol.* 36:39–53

Dury CM, Ristow GH. 1997. Radial segregation in a two-dimensional rotating drum. *J. Phys. I, France* 7:737–45

Elperin T, Vikhansky A. 1998a. Granular flow in a rotating cylindrical drum. *Europhys. Lett.* 42:619–23

Elperin T, Vikhansky A. 1998b. Kinematics of the mixing of granular materials in slowly rotating containers. *Europhys. Lett.* 43:17–22

Epstein IR, Showalter K. 1996. Nonlinear chemical dynamics: oscillations, patterns, and chaos. *J. Phys. Chem.* 100(31):13132–47

Fan LT, Chen YM, Lai FS. 1990. Recent developments in solids mixing. *Powder Technol.* 61:255–87

Fisher RA. 1926. On the capillary forces in an ideal soil. *J. Agric. Sci.* 16:491–505

Goldenfeld N, Kadanoff LP. 1999. Simple lessons from complexity. *Science* 284:87–89

Hehl M, Kroger H, Helmrich H, Schugerl K. 1978. Longitudinal mixing in horizontal drum reactors. *Powder Technol.* 20:29–37

Henein H, Brimacomble JK, Watkinson AP. 1983. Experimental study of transverse bed motion in rotary kilns. *Metal. Trans. B* 14:191–205

Hill KM, Kakalios J. 1995. Reversible axial segregation of rotating granular media. *Phys. Rev. E* 52:4393–400

Hill KM, Caprihan A, Kakalios J. 1997. Bulk segregation in a rotated granular material measured by magnetic resonance imaging. *Phys. Rev. Lett.* 78:50–53

Hill KM, Khakhar DV, Gilchrist JF, McCarthy JJ, Ottino JM. 1999a. Segregation-driven organization in chaotic granular flows. *Proceedings of the National Academy of Sciences* 96:11701–706

Hill KM, Gilchrist JF, Khakhar DV, McCarthy JJ, Ottino JM. 1999b. Mixing of granular materials: a test-bed dynamical system for pattern formation. *Int. J. Bifurc. Chaos* 9:1467–84

Hirschfeld D, Rapaport DC. 1997. Molecular dynamics studies of grain segregation in a sheared flow. *Phys. Rev. E* 56:2012–18

Hirschfelder JO, Curtiss CF, Bird RB. 1954. *Molecular Theory of Gases and Liquids.* New York: Wiley & Sons 1219 pp.

Hogg R, Cahn DS, Healy TW, Fuerstenau DW. 1966. Diffusional mixing in an ideal system. *Chem. Eng. Sci.* 21:1025–38

Hogg R, Fuerstenau DW. 1972. Transverse mixing in rotating cylinders. *Powder Technol.* 6:139–48

Hornbaker D, Albert R, Albert I, Barabasi AL, Schieffer P. 1997. What keeps sandcastles standing. *Nature* 387:765–67

Hsiau SS, Hunt ML. 1996. Granular thermal diffusion in flows of binary-sized mixtures. *Acta Mech.* 114:121–37

Inoue I, Yamaguchi K, Sato K. 1970. Motion of a particle and mixing process in a horizontal drum mixer, *Kagaku Kogaku* 34:1323–30

Jackson R. 1986. Some features of the flow of granular materials and aerated granular materials. *J. Rheol.* 30:907–30

Jaeger HM, Nagel SR. 1992. The physics of the granular state. *Science* 255:1523–31

Jaeger HM, Nagel SR, Behringer RP. 1996a. Granular solids, liquids, and glasses. *Rev. Mod. Phys.* 68:1259–73

Jaeger HM, Nagel SR, Behringer RP. 1996b. The physics of granular materials. *Phys. Today* 49:32–38

Jenkins JT, Mancini F. 1989. Kinetic theory for binary mixtures of smooth, nearly elastic spheres. *Phys. Fluids A* 1:2050–57

Johanson JR. 1978. Particle segregation and what to do about it. *Chem. Eng.* 85:183–88

Johnson PC, Jackson R. 1987. Frictional-collisional constitutive relations for granular materials, with application to plane shearing. *J. Fluid Mech.* 176:67–93

Julien R, Meakin P. 1990. A mechanism for particle size segregation in three dimensions. *Nature* 344:425–27

Khakhar DV, McCarthy JJ, Gilchrist JF, Ottino JM. 1999a. Chaotic mixing of granular materials in 2D tumbling mixers. *CHAOS* 9:195–205

Khakhar DV, McCarthy JJ, Ottino JM. 1999b. Mixing and segregation of granular materials in chute flows. *CHAOS* 9:594–610

Khakhar DV, McCarthy JJ, Ottino JM. 1997a. Radial segregation of materials in rotating cylinders. *Phys. Fluids* 9:3600–14

Khakhar DV, McCarthy JJ, Shinbrot T, Ottino JM. 1997b. Transverse flow and mixing of granular materials in a rotating cylinder. *Phys. Fluids* 9:31–43

Knight JB, Jaeger HM, Nagel SR. 1993. Vibration induced granular segregation in granular media: the convection connection. *Phys. Rev. Lett.* 70:3728–31

Kincaid JM, Cohen EGD, de Haro ML. 1987. The Enskog theory for multicomponent mixtures. IV. Thermal diffusion. *J. Chem. Phys.* 86:963–75

Koeppe JP, Enz M, Kakalios J. 1998. Phase diagram for avalanche stratification of granular media. *Phys. Rev. E* 58:R4104

Lacey PM. 1954. Developments in the theory of particle mixing. *J. Appl. Chem.* 4:257–68

Lehmberg J, Hehl M, Schugerl K. 1977. Transverse mixing and heat transfer in horizontal rotary drum reactors. *Powder Technol.* 18:149–63

Levitan B. 1998. Segregation and coarsening of a granular mixture in a rotating tube. *Physica A* 249:386–90

Lian G, Thornton C, Adams MJ. 1993. A theoretical study of liquid bridge forces between two rigid spherical bodies. *J. Colloid Int. Sci.* 161:138–47

Lian G, Thornton C, Adams MJ. 1998. Discrete particle simulation of agglomerate impact coalescence. *Chem. Eng. Sci.* 53:3381–91

Lun CKK, Savage SB, Jeffrey DJ, Chepurniy N. 1984. Kinetic theories for granular flow: inelastic particles in Couette flow and slightly inelastic particles in a general flow field. *J. Fluid Mech.* 140:223–56

Makse HA, Havlin S, King PR, Stanley HE. 1997. Spontaneous stratification in granular mixtures. *Nature* 386:379–81

McCarthy JJ. 1998. *Mixing, segregation, and flow of granular materials.* PhD thesis. Evanston, Ill: Northwestern Univ.

McCarthy JJ, Ottino JM. 1997. Particle dynamics simulation: a hybrid technique applied to granular mixing. *Powder Technol.* 97:91–99

McCarthy JJ, Ottino JM. 1998. A computational study of granular mixing: the effect of particle cohesion. *Proceedings of the Topical Conference on Advanced Technologies for Particle Processing, Amer. Inst. Chem. Eng. Annual Meeting, Miami Beach, FL.* 552–58

McCarthy JJ, Shinbrot T, Metcalfe G, Wolf JE, Ottino JM. 1996. Mixing of granular materials in slowly rotated containers. *AIChE J.* 42:3351–63

Meloy TP, Mani BP, Clark NN. 1986. Particle shape analysis and separation techniques: a critical review. *J. Powder Bulk Solids Technol.* 10:15–20

Metcalfe G, Shattuck M. 1996. Pattern formation during mixing and segregation of flowing granular materials. *Physica A* 233:709–17

Metcalfe G, Shinbrot T, McCarthy JJ, Ottino JM. 1995. Avalanche mixing of granular solids. *Nature* 374:39–41

Mindlin RD. 1949. Compliance of elastic bodies in contact. *J. Appl. Mech.* 16:256–70

Muzzio FJ, Robinson P, Wightman C, Brone D. 1997. Sampling practices in powder blending. *Int. J. Pharm.* 155:153–78

Nakagawa M. 1994. Axial segregation of granular flows in a horizontal rotating cylinder. *Chem. Eng. Sci.* 49:2540–44

Nakagawa M, Altobelli, SA, Caprihan A, Fukushima E, Jeong EK. 1993. Non-invasive measurements of granular flows by magnetic resonance imaging. *Exp. Fluids.* 16:54–60

Nienow AW, Edwards MF, Harnby N. 1985. In *Mixing in the Process Industries,* ed. N Harnby, MF Edwards, AW Nienow, p. 1. London: Butterworths.

Nityanand N, Manley B, Henein H. 1986. An analysis of radial segregation for different sized spherical solids in rotary cylinders. *Metal. Trans. B* 17:247–57

Onuki A. 1997. Phase transitions of fluids in shear flow. *J. Phys-Condens. Matter* 9:6119–57

Ottino JM. 1989. *The kinematics of mixing: stretching, chaos, and transport.* Cambridge, UK: Cambridge Univ. Press

Ottino JM. 1990. Mixing, chaotic advection, and turbulence. *Annu. Rev. Fluid Mech.* 22:207–54

Ottino JM, Shinbrot T. 1999. *Comparing extremes: mixing of fluids, mixing of solids.* In *Mixing: Chaos and Turbulence,* ed. H. Chaté, E Villermaux, J-M Chomaz, pp. 163–86. NATO Sci. Ser. New York: Kluwer Acad./Plenum

Pierrat P, Caram HS. 1997. Tensile strength of wet granular materials. *Powder Technol.* 91:83–93

Polhausen E. 1921. Zur näherungsweisen Intergration der Differentialgleichung der laminaren Grenzschicht. *Z. Angewal Mathemat. Mechan.* 1:115–21

Poux M, Fayolle P, Bertrand J, Bridoux D, Bousquet J. 1991. Powder mixing: some practical rules applied to agitated systems. *Powder Technol.* 68:213–34

Prigozhin L, Kalman H. 1998. Radial mixing and segregation of a binary mixture in a rotating drum: model and experiment. *Phys. Rev. E* 57:2073–80

Rajchenbach J. 1990. Flow in powders: from discrete avalanches to continuous regime. *Phys. Rev. Lett.* 65:2221–24

Rajchenbach J, Clement E, Duran J. 1995. Experiments in model granular media: a study of gravity flows. In *Fractal Aspects of Materials,* ed. F Family, P Meakin, B Sapoval, R Wool, p. 525. Pittsburgh: MRS Symp.

Rao SJ, Bhatia SK, Khakhar DV. 1991. Axial transport of granular solids in rotating cylinders. Part 2. Experiments in a non-flow system. *Powder Technol.* 67:153–62

Ristow GH. 1994. Particle mass segregation in a two-dimensional rotating drum. *Europhys. Lett.* 28:97–101

Rosato A, ed. 1999. *Segregation in Granular Flows. IUTAM Symp., June 5–10, Cape May, NJ.* Dordrecht, The Netherlands: Kluwer

Rosato A, Prinze F, Standburg KJ, Svendsen R. 1987. Why Brazil nuts are on top: size segregation of particulate matter by shaking. *Phys. Rev. Lett.* 58:1038–40

Savage SB. 1993. Disorder, diffusion and structure formation in granular flow. In *Disorder and Granular Media,* ed. D. Bideau, A Hansen, pp. 255–85. Amsterdam: Elsevier

Savage SB, Lun CKK. 1988. Particle size segregation in inclined chute flow of cohesionless granular slids. *J. Fluid Mech.* 189:311–35

Schafer J, Dippel S, Wolf DE. 1996. Force schemes in simulation of granular materials. *J. Physique I* 6:5–20

Scott AM, Bridgwater J. 1976. Self-diffusion of spherical particles in a simple shear apparatus. *Powder Technol.* 14:177–83

Shinbrot T, Alexander AW, Muzzio FJ. 1999. Spontaneous chaotic mixing. *Nature* 397:675–78

Thornton C, Yin KK, Adams MJ. 1996. Numerical simulation of the impact fracture and fragmentation of agglomerates. *J. Phys. D* 29:424–35

Wagner AJ, Yeomans JM. 1998. Breakdown of scale invariance in the coarsening of phase separating binary fluids. *Phys. Rev. Lett.* 80:1429–32

Walton OR. 1993. Numerical simulation of inclined chute flows of monodisperse, inelastic, frictional spheres. *Mech. Mater.* 16:239–47

Wes GWJ, Drinkenburg AAH, Stemerding S. 1976. Solids mixing and residence time distributions in a horizontal rotary drum reactor. *Powder Technol.* 13:177–84

Wightman C, Muzzio FJ. 1998a. Mixing of granular material in a drum mixer undergoing rotational and rocking motions. I. Uniform particles. *Powder Technol.* 98:113–24

Wightman C, Muzzio FJ. 1998b. Mixing of granular material in a drum mixer undergoing rotational and rocking motions. II. Segregating particles. *Powder Technol.* 98:125–34

Williams JC. 1963. The segregation of powders and granular materials. *Fuel Soc. J.* 14:29–34

Williams JC. 1976. The segregation of particulate materials: a review. *Powder Technol.* 15:246–51

Zik O, Levine D, Lipson SG, Shtrikman S, Stavans J. 1994. Rotationally induced segregation of granular materials. *Phys. Rev. Lett.* 73:644–47

Figure 9 Computed Poincaré sections for circular, elliptical, and square mixer simulated by using the model with no particle diffusion. The layer thickness in all cases is $\delta_0/L = 0.05$ (from Khakhar et al 1999a, reproduced with permission).
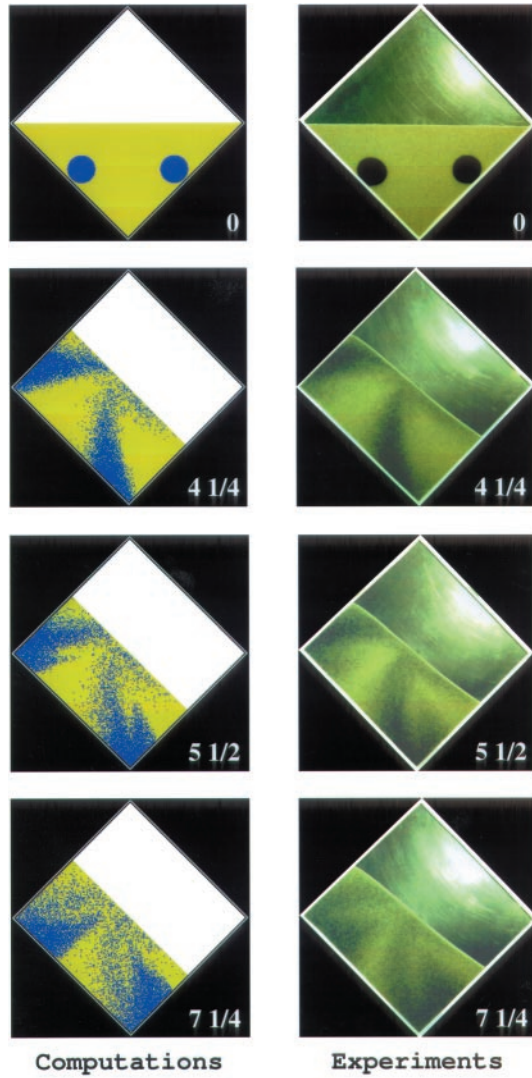
Figure 10 Mixing of tracer particles in a container with a square cross section. Shown is a comparison of an experiment with colored glass beads (*right*) and a simulation using the model (*left*). The number of rotations for each image is listed in the corner (from Khakhar et al 1999a, reproduced with permission).
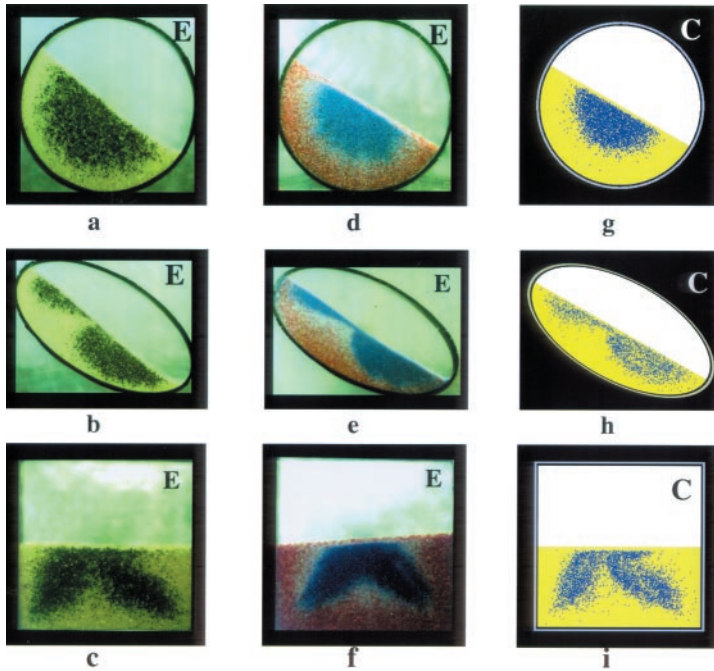
Figure 13 The competition between mixing and segregation resulting in equilibrium patterns is shown for mixtures of particles differing in density (*column 1*) and size (*column 2*) for mixers of different shapes. The mixers are half filled with particles. Model predictions for different-density particles with equal sizes are based on a model incorporating density-driven segregation (see text section 6) and chaotic advection (see text section 7) are shown in *column 3* (adapted from KM Hill et al 1999a).
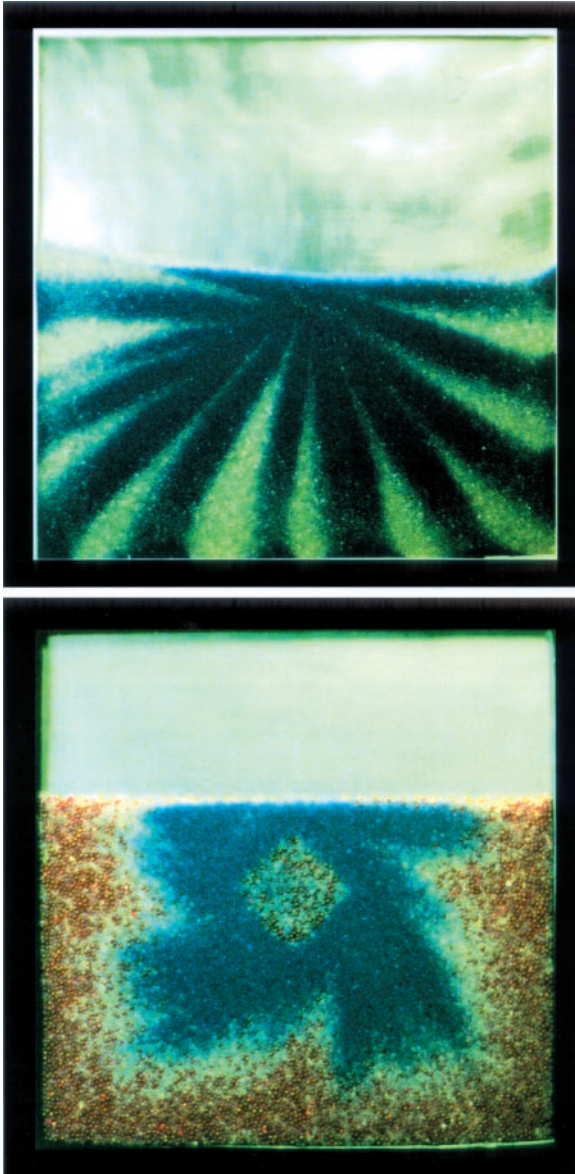
Figure 14 (a) Streak pattern produced by an instability for mixtures of differently sized glass beads. The pattern is produced for fill levels just > 50% and results from the different flow velocities for the smaller and larger particles in the layer. (b) Increasing the filling results in a radically different structure (from Hill et al 1999a).